



A priori and a posteriori analysis for a locking-free low order quadrilateral hybrid finite element for Reissner–Mindlin plates

Carsten Carstensen^{a,b}, Xiaoping Xie^{c,*}, Guozhu Yu^c, Tianxiao Zhou^d

^a Institut für Mathematik, Humboldt Universität zu Berlin, Unter den Linden 6, 10099 Berlin, Germany

^b Department of Computational Science and Engineering, Yonsei University, 120-749 Seoul, South Korea

^c School of Mathematics, Sichuan University, Chengdu 610064, China

^d Aeronautical Computing Technique Research Institute, Xi'an 710068, China

ARTICLE INFO

Article history:

Received 24 March 2010

Received in revised form 15 June 2010

Accepted 30 June 2010

Available online 14 July 2010

AMS subject classification:

65N12

65N15

65N30

Keywords:

Reissner–Mindlin plate

Hybrid finite element

Quadrilateral element

A priori error

A posteriori error

ABSTRACT

This paper proposes a quadrilateral finite element method of the lowest order for Reissner–Mindlin (R–M) plates on the basis of Hellinger–Reissner variational principle, which includes variables of displacements, shear stresses and bending moments. This method uses continuous piecewise isoparametric bilinear interpolation for the approximation of transverse displacement and rotation. The piecewise-independent shear stress/bending moment approximation is constructed by following a self-equilibrium criterion and a shear-stress-enhanced condition. A priori and reliable a posteriori error estimates are derived and shown to be uniform with respect to the plate thickness t . Numerical experiments confirm the theoretical results.

© 2010 Elsevier B.V. All rights reserved.

1. Introduction

The Reissner–Mindlin (R–M) model describes the deformation of an isotropic homogeneous plate, with the thickness t , subject to a transverse loading g . More precisely, for a clamped R–M plate, the rotation β of the fibers normal to the midplane and the transverse displacement w of the midplane Ω minimize over $H_0^1(\Omega)^2 \times H_0^1(\Omega)$ the plate energy

$$\Pi(\beta, w) = \frac{1}{2} \int_{\Omega} \epsilon(\beta) : \mathcal{D}\epsilon(\beta) \, d\mathbf{x} + \frac{\lambda t^{-2}}{2} \int_{\Omega} |\nabla w - \beta|^2 \, d\mathbf{x} - \int_{\Omega} g w \, d\mathbf{x}. \quad (1.1)$$

Here $\Omega \in \mathbb{R}^2$ is, for simplicity, assumed to be a convex polygon. $\epsilon(\beta)$ denotes the symmetric part of the gradient of β . $\mathcal{D}\mathbf{Q}$, for any 2×2 symmetric matrix \mathbf{Q} is defined by

$$\mathcal{D}\mathbf{Q} = \frac{E}{12(1-\nu^2)} [(1-\nu)\mathbf{Q} + \nu \text{tr}(\mathbf{Q})\mathbf{I}],$$

$\mathbf{Q} : \mathbf{M} = \sum_{1 \leq i, j \leq 2} Q_{ij} M_{ij}$ for any two 2×2 matrices \mathbf{Q} and \mathbf{M} , and $\lambda = \frac{\kappa E}{2(1+\nu)}$, with Young's modulus E , Poisson's ratio $0 < \nu < \frac{1}{2}$, and the shear correction factor $\kappa = \frac{5}{6}$.

To avoid the C^1 -continuity difficulty, the R–M plate today becomes the dominant two-dimensional model used to calculate the bending of a thick/thin three-dimensional plate.

Standard low-order finite elements usually fail the approximation for a plate thickness t close to zero (cf. [2,29]). The reason for this phenomenon, called shear locking, is that when the plate thickness becomes small, the shear energy term degenerates to impose (within the limit $t = 0$) the Kirchhoff constraint, which is too severe for low-order elements.

To avoid the shear locking difficulty, the most common approach is to modify the variational formulation so as to weaken the Kirchhoff constraint, where some reduction operator is used [5,9,12,15,18,19,25,26,28,31,32,36,46]. An alternative approach is to employ an equivalent formulation of the original problem. For example, in [17], the Helmholtz decomposition was used which involves two additional unknowns. In [1], an equivalent mixed formulation was introduced by decomposing the bending moment and by dualizing its symmetry. One can also work with the standard variational formulation and use more expensive continuous

* Corresponding author.

E-mail addresses: cc@math.hu-berlin.de (C. Carstensen), xpniec@gmail.com (X. Xie), yuguozhumail@yahoo.com.cn (G. Yu).

finite elements [39,41] for the discretization. One may also refer to [24,27,30,35] for stabilization methods, to [13,20] for least-square methods and to [3,4,16,44] for discontinuous Galerkin methods.

When introducing the shear stress vector $\gamma = \lambda t^{-2}(\nabla w - \beta)$ and the bending moment tensor $\mathbf{M} = -\mathcal{D}\epsilon(\beta)$, the Euler equations for the Reissner–Mindlin plate problem (1.1) read as:

$$\operatorname{div} \mathbf{M} - \gamma = 0 \text{ in } \Omega, \quad (1.2)$$

$$\operatorname{div} \gamma + g = 0 \text{ in } \Omega, \quad (1.3)$$

$$\mathbf{M} + \mathcal{D}\epsilon(\beta) = 0 \text{ in } \Omega, \quad (1.4)$$

$$\gamma - \lambda t^{-2}(\nabla w - \beta) = 0 \text{ in } \Omega, \quad (1.5)$$

$$w = 0, \beta = 0 \text{ on } \partial\Omega. \quad (1.6)$$

This system leads to some alternative mixed/hybrid finite element discretization on the basis of the Hellinger–Reissner energy functional

$$\Pi = \frac{1}{2} a(\mathbf{M}, \gamma; \mathbf{M}, \gamma) + b(\mathbf{M}, \gamma; w, \beta) + \int_{\Omega} g w \, dx, \quad (1.7)$$

where the bilinear forms

$$a(\cdot, \cdot; \cdot, \cdot) : (L^2(\Omega)_{\text{sym}}^{2 \times 2} \times L^2(\Omega)^2) \times (L^2(\Omega)_{\text{sym}}^{2 \times 2} \times L^2(\Omega)^2) \rightarrow \mathbb{R},$$

$$b(\cdot, \cdot; \cdot, \cdot) : (L^2(\Omega)_{\text{sym}}^{2 \times 2} \times L^2(\Omega)^2) \times (H_0^1(\Omega) \times H_0^1(\Omega)^2) \rightarrow \mathbb{R}$$

are defined by

$$a(\mathbf{M}, \gamma; \mathbf{Q}, \tau) := \int_{\Omega} \mathbf{M} : \mathcal{D}^{-1} \mathbf{Q} \, dx + \frac{t^2}{\lambda} \int_{\Omega} \gamma \cdot \tau \, dx, \quad (1.8)$$

$$b(\mathbf{Q}, \tau; v, \zeta) := \int_{\Omega} \mathbf{Q} : \epsilon(\zeta) \, dx - \int_{\Omega} \tau \cdot (\nabla v - \zeta) \, dx. \quad (1.9)$$

The main features of the mixed/hybrid formulations above are as follows:

- C^0 continuity is required for kinematic variables.
- C^{-1} or L^2 continuity is required for bending moment and shear stress variables. This ensures the use of piecewise independent approximation of the bending moment and shear stress variables, and will finally lead to a discretization system with the only unknowns being displacements.
- With some rational choice of bending moment and shear stress approximation, one can derive locking-free methods without the introduction of some reduction operator.

This work shall propose and analyze a low order locking-free quadrilateral hybrid finite element method for the R–M plate based on the functional (1.7). We use continuous isoparametric bilinear interpolation for the approximation of transverse displacement w and rotation β , and impose, on the approximation of bending moment \mathbf{M} and shear stress γ , the bending equilibrium relation (1.2) as well as a shear-stress-enhanced condition. It should be mentioned that in [7] a hybrid quadrilateral element was constructed and shown numerically to be locking-free, where continuous isoparametric bilinear displacement interpolation and equilibrium bending moment/shear stress approximation plus the same technique of shear interpolation as in the element MITC4 [9] were used.

We arrange the rest of this paper as follows. In Section 2 we provide the weak formulation of the model (1.2)–(1.6) and show its well posedness. Section 3 proves locking-free a priori error estimates for finite element discretization under some general assumptions. Section 4 is devoted to construction of locking-free quadrilateral finite element method. We derive residual-based a posteriori error estimates which are reliable in Section 5. Finally, we give some numerical results in Section 6 to verify the theoretical results.

2. Weak formulations and well posedness

First we introduce some notations. Let $H^k(T)$ be the usual Sobolev space consisting of functions defined on T with all derivatives of order up to k square-integrable; $H^0(T) = L^2(T)$, $H_0^1(T) := \{v \in H^1(T) : v|_{\partial T} = 0\}$. We denote the norm on $H^k(T; X)$ by $\|\cdot\|_{k,T} := \left(\sum_{0 \leq j \leq k} |\cdot|_{j,T}^2\right)^{1/2}$ with $|\cdot|_{k,T}$ the semi-norm derived from the partial derivatives of order equal to k . When there is no conflict, we may abbreviate $\|\cdot\|_{k,\Omega}$ and $|\cdot|_{k,\Omega}$ respectively to $\|\cdot\|_k$ and $|\cdot|_k$. Let $L^2(\Omega)_{\text{sym}}^{2 \times 2}$ be the space of square-integrable symmetric tensors with the norm $\|\cdot\|_0$ defined by $\|\mathbf{Q}\|_0^2 := \int_{\Omega} \mathbf{Q} : \mathbf{Q} \, dx$. We denote by $P_k(T)$ and $P_{k,k}$ the set of polynomials of degree less than or equal to k and the set of polynomials of degree less than or equal to k in each variable, respectively.

For convenience, throughout the paper we use the notation $a \lesssim b$ to represent that there exists a generic positive constant C , independent of the mesh parameter h and the plate thickness t , such that $a \leq Cb$. We also abbreviate $a \lesssim b \lesssim a$ as $a \approx b$.

We set $\mathbb{M} := L^2(\Omega)_{\text{sym}}^{2 \times 2}$, $\Gamma := L^2(\Omega)^2$, $W := H_0^1(\Omega)$, $\Theta := H_0^1(\Omega)^2$. Then the variational formulation of Eqs. (1.2)–(1.6) reads: Find $(\mathbf{M}, \gamma, w, \beta) \in \mathbb{M} \times \Gamma \times W \times \Theta$ such that

$$a(\mathbf{M}, \gamma; \mathbf{Q}, \tau) + b(\mathbf{Q}, \tau; w, \beta) = 0 \text{ for all } (\mathbf{Q}, \tau) \in \mathbb{M} \times \Gamma, \quad (2.1)$$

$$b(\mathbf{M}, \gamma; v, \zeta) = - \int_{\Omega} g v \, dx \text{ for all } (v, \zeta) \in W \times \Theta \quad (2.2)$$

with $a(\cdot, \cdot; \cdot, \cdot)$ and $b(\cdot, \cdot; \cdot, \cdot)$ from (1.8) and (1.9).

For our analysis we introduce the following norms for the space pairs $\mathbb{M} \times \Gamma$ and $W \times \Theta$:

$$\|(\mathbf{Q}, \tau)\|_{\mathbb{M} \times \Gamma} := \|\mathbf{Q}\|_0 + t\|\tau\|_0 + \|\tau\|_{-1} + |\tau|_{\star} \text{ for all } (\mathbf{Q}, \tau) \in \mathbb{M} \times \Gamma, \quad (2.3)$$

$$\|(v, \zeta)\|_{W \times \Theta} := \|\zeta\|_1 + \|v\|_1 \text{ for all } (v, \zeta) \in W \times \Theta, \quad (2.4)$$

where

$$\|\tau\|_{-1} := \sup_{\zeta \in H_0^1(\Omega)^2} \frac{\int_{\Omega} \tau \cdot \zeta \, dx}{\|\zeta\|_1}, \quad |\tau|_{\star} := \sup_{v \in H_0^1(\Omega)} \frac{\int_{\Omega} \tau \cdot \nabla v \, dx}{\|v\|_1}.$$

With the above norms, we easily have the following uniform boundedness: for all $\mathbf{Q}, \mathbf{M} \in \mathbb{M}$, $\gamma, \tau \in \Gamma$, $v \in W$, $\zeta \in \Theta$, it holds

$$|a(\mathbf{M}, \gamma; \mathbf{Q}, \tau)| \lesssim \|(\mathbf{M}, \gamma)\|_{\mathbb{M} \times \Gamma} \|(\mathbf{Q}, \tau)\|_{\mathbb{M} \times \Gamma}, \quad (2.5)$$

$$|b(\mathbf{Q}, \tau; v, \zeta)| \lesssim \|(\mathbf{Q}, \tau)\|_{\mathbb{M} \times \Gamma} \|(v, \zeta)\|_{W \times \Theta}, \quad (2.6)$$

$$\left| \int_{\Omega} g v \, dx \right| \leq \|g\|_{-1} \|v\|_1 \leq \|g\|_{-1} \|(v, \zeta)\|_{W \times \Theta}. \quad (2.7)$$

Define the kernel subspace

$$Z := \{(\mathbf{Q}, \tau) \in \mathbb{M} \times \Gamma : b(\mathbf{Q}, \tau; v, \zeta) = 0 \text{ for all } (v, \zeta) \in W \times \Theta\}.$$

Then we have the kernel coercivity result.

Lemma 2.1. For all $(\mathbf{Q}, \tau) \in Z$,

$$\|(\mathbf{Q}, \tau)\|_{\mathbb{M} \times \Gamma}^2 \lesssim a(\mathbf{Q}, \tau; \mathbf{Q}, \tau). \quad (2.8)$$

Proof. We already have

$$\|\mathbf{Q}\|_0^2 + t\|\tau\|_0^2 \lesssim a(\mathbf{Q}, \tau; \mathbf{Q}, \tau) \text{ for all } (\mathbf{Q}, \tau) \in \mathbb{M} \times \Gamma.$$

For $(\mathbf{Q}, \tau) \in Z$, it holds

$$\int_{\Omega} \mathbf{Q} : \epsilon(\zeta) \, dx + \int_{\Omega} \tau \cdot \zeta \, dx = 0 \text{ for all } \zeta \in \Theta \quad (2.9)$$

and

$$\int_{\Omega} \boldsymbol{\tau} \cdot \nabla v \, d\mathbf{x} = 0 \quad \text{for all } v \in W. \quad (2.10)$$

The equality (2.9) indicates

$$\|\boldsymbol{\tau}\|_{-1,\Omega} = \sup_{\zeta \in H_0^1(\Omega)^2} \frac{-\int_{\Omega} \mathbf{Q} : \boldsymbol{\epsilon}(\zeta) \, d\mathbf{x}}{\|\zeta\|_{1,\Omega}} \leq \|\mathbf{Q}\|_{0,\Omega},$$

and the equality (2.10) yields $|\boldsymbol{\tau}|_{\star} = 0$. Therefore, the kernel coercivity (2.8) follows. \square

We have the following inf–sup inequality.

Lemma 2.2. For all $(v, \zeta) \in W \times \Theta$,

$$\|(v, \zeta)\|_{W \times \Theta} \lesssim \sup_{(\mathbf{Q}, \boldsymbol{\tau}) \in \mathbb{M} \times \Gamma} \frac{b(\mathbf{Q}, \boldsymbol{\tau}; v, \zeta)}{\|(\mathbf{Q}, \boldsymbol{\tau})\|_{\mathbb{M} \times \Gamma}}. \quad (2.11)$$

Proof. The desired result follows from

$$\|\zeta\|_1 \approx \|\boldsymbol{\epsilon}(\zeta)\|_0 \leq \sup_{\mathbf{Q} \in \mathbb{M}} \frac{\int_{\Omega} \mathbf{Q} : \boldsymbol{\epsilon}(\zeta) \, d\mathbf{x}}{\|\mathbf{Q}\|_0}$$

and

$$\|v\|_1 \approx \|\nabla v\|_0 \leq \sup_{\boldsymbol{\tau} \in \Gamma} \frac{\int_{\Omega} \boldsymbol{\tau} \cdot \nabla v \, d\mathbf{x}}{\|\boldsymbol{\tau}\|_0} \lesssim \sup_{\boldsymbol{\tau} \in \Gamma} \frac{\int_{\Omega} \boldsymbol{\tau} \cdot \nabla v \, d\mathbf{x}}{t\|\boldsymbol{\tau}\|_0 + \|\boldsymbol{\tau}\|_{-1} + |\boldsymbol{\tau}|_{\star}}$$

for $v \in W$ and $\zeta \in \Theta$. \square

In view of the conditions (2.5)–(2.11), and from the theory for saddle-point problems [14,18], we obtain the following well posedness result.

Theorem 2.1. The problem (2.1) and (2.2) admits a unique solution $(\mathbf{M}, \boldsymbol{\gamma}, w, \boldsymbol{\beta}) \in \mathbb{M} \times \Gamma \times W \times \Theta$ and it holds

$$\|(\mathbf{M}, \boldsymbol{\gamma})\|_{\mathbb{M} \times \Gamma} + \|(w, \boldsymbol{\beta})\|_{W \times \Theta} \lesssim \|g\|_{-1}. \quad (2.12)$$

Moreover, the bilinear form $A(\cdot; \cdot) : (\mathbb{M} \times \Gamma \times W \times \Theta) \times (\mathbb{M} \times \Gamma \times W \times \Theta) \rightarrow \mathbb{R}$, defined by

$$A(\mathbf{M}, \boldsymbol{\gamma}, w, \boldsymbol{\beta}; \mathbf{Q}, \boldsymbol{\tau}, v, \zeta) := a(\mathbf{M}, \boldsymbol{\gamma}; \mathbf{Q}, \boldsymbol{\tau}) + b(\mathbf{Q}, \boldsymbol{\tau}; w, \boldsymbol{\beta}) + b(\mathbf{M}, \boldsymbol{\gamma}; v, \zeta) \quad (2.13)$$

for all $(\mathbf{M}, \boldsymbol{\gamma}, w, \boldsymbol{\beta}), (\mathbf{Q}, \boldsymbol{\tau}, v, \zeta) \in \mathbb{M} \times \Gamma \times W \times \Theta$, provides an isomorphism between $\mathbb{M} \times \Gamma \times W \times \Theta$ and its dual with equivalent norms

$$\|(\mathbf{M}, \boldsymbol{\gamma})\|_{\mathbb{M} \times \Gamma} + \|(w, \boldsymbol{\beta})\|_{W \times \Theta} \approx \sup_{(\mathbf{Q}, \boldsymbol{\tau}, v, \zeta) \in \mathbb{M} \times \Gamma \times W \times \Theta} \frac{A(\mathbf{M}, \boldsymbol{\gamma}, w, \boldsymbol{\beta}; \mathbf{Q}, \boldsymbol{\tau}, v, \zeta)}{\|(\mathbf{Q}, \boldsymbol{\tau})\|_{\mathbb{M} \times \Gamma} + \|(v, \zeta)\|_{W \times \Theta}} \quad (2.14)$$

for $(\mathbf{M}, \boldsymbol{\gamma}, w, \boldsymbol{\beta}) \in \mathbb{M} \times \Gamma \times W \times \Theta$.

To get further regularity of the solution $(\mathbf{M}, \boldsymbol{\gamma}, w, \boldsymbol{\beta})$, we introduce a weak problem: find $(w, \boldsymbol{\beta}, \boldsymbol{\gamma}) \in W \times \Theta \times \Gamma$ such that

$$\int_{\Omega} \boldsymbol{\epsilon}(\boldsymbol{\beta}) : \mathcal{D}\boldsymbol{\epsilon}(\zeta) \, d\mathbf{x} + \int_{\Omega} \boldsymbol{\gamma} \cdot (\nabla v - \zeta) \, d\mathbf{x} = \int_{\Omega} g v \, d\mathbf{x} \quad \text{for all } v \in W, \zeta \in \Theta, \quad (2.15)$$

$$\int_{\Omega} \boldsymbol{\tau} \cdot (\nabla w - \boldsymbol{\beta}) \, d\mathbf{x} - \frac{t^2}{\lambda} \int_{\Omega} \boldsymbol{\gamma} \cdot \boldsymbol{\tau} \, d\mathbf{x} = 0 \quad \text{for all } \boldsymbol{\tau} \in \Gamma. \quad (2.16)$$

Remark 2.1. In fact, the variational formulations (2.1) and (2.2) can also be derived from (2.15) and (2.16) by introducing the bending moment tensor $\mathbf{M} = -\mathcal{D}\boldsymbol{\epsilon}(\boldsymbol{\beta})$, which yields

$$\int_{\Omega} \mathbf{M} : \mathcal{D}^{-1} \mathbf{Q} \, d\mathbf{x} + \int_{\Omega} \mathbf{Q} : \boldsymbol{\epsilon}(\boldsymbol{\beta}) \, d\mathbf{x} = 0 \quad \text{for all } \mathbf{Q} \in \mathbb{M}.$$

We recall the following result (see [5,17]).

Lemma 2.3. The problem (2.15) and (2.16) admits a unique solution with

$$\|w\|_2 + \|\boldsymbol{\beta}\|_2 + \|\boldsymbol{\gamma}\|_0 + t\|\boldsymbol{\gamma}\|_1 \lesssim \|g\|_0. \quad (2.17)$$

In addition, if Ω is a smoothly bounded domain and $g \in H^1(\Omega)$, then it holds

$$\|w\|_3 \lesssim \|g\|_1. \quad (2.18)$$

With the above lemma, we obtain some further results.

Theorem 2.2. Let $(w, \boldsymbol{\beta}, \boldsymbol{\gamma}) \in W \times \Theta \times \Gamma$ be the solution of the problem (2.15) and (2.16). Then the following three conclusions (i)–(iii) hold.

- (i) The quadruple $(\mathbf{M} = -\mathcal{D}\boldsymbol{\epsilon}(\boldsymbol{\beta}), \boldsymbol{\gamma}, w, \boldsymbol{\beta}) \in \mathbb{M} \times \Gamma \times W \times \Theta$ is the unique solution of the problem (2.1) and (2.2);
- (ii) If $\mathbf{M} \in \mathbf{H}(\mathbf{div}, \Omega) := \{\mathbf{Q} \in L^2(\Omega)_{\text{sym}}^{2 \times 2} : \mathbf{div} \mathbf{Q} \in L^2(\Omega)^2\}$, then the equilibrium relation (1.2) holds;
- (iii) Provided that $g \in L^2(\Omega)$, regularity holds in the sense of

$$\|w\|_2 + \|\boldsymbol{\beta}\|_2 + \|\mathbf{M}\|_1 + \|\boldsymbol{\gamma}\|_0 + t\|\boldsymbol{\gamma}\|_1 \lesssim \|g\|_0. \quad (2.19)$$

Proof

- (i) Existence and uniqueness follows from Theorem 2.1. It will be shown that $(\mathbf{M}, \boldsymbol{\gamma}, w, \boldsymbol{\beta})$ satisfies (2.1) and (2.2). In fact, from (2.16) and $\mathbf{M} = -\mathcal{D}\boldsymbol{\epsilon}(\boldsymbol{\beta})$, Eq. (2.2) is obvious. On the other hand, by $\mathcal{D}^{-1} \mathbf{M} = -\boldsymbol{\epsilon}(\boldsymbol{\beta})$ and (2.16), one obtains (2.1).
- (ii) From (2.2) we have

$$\int_{\Omega} \mathbf{M} : \boldsymbol{\epsilon}(\zeta) \, d\mathbf{x} + \int_{\Omega} \boldsymbol{\gamma} \cdot \zeta \, d\mathbf{x} = 0 \quad \text{for all } \zeta \in H_0^1(\Omega)^2.$$

Then (1.2) follows from integration by parts.

- (iii) The regularity result (2.19) follows from (2.17) and $\mathbf{M} = -\mathcal{D}\boldsymbol{\epsilon}(\boldsymbol{\beta})$. \square

3. General assumptions and locking-free a priori error estimates for finite element discretization

Let T_h be a regular family of finite element subdivisions of the polygonal domain Ω . Let $\mathbb{M}_h \subset \mathbb{M}$, $\Gamma_h \subset \Gamma$, $W_h \subset W$, and $\Theta_h \subset \Theta$ be finite dimensional spaces for the bending moment, shear stress, transverse displacement, and rotation approximation. Then the corresponding finite element scheme for the problem (2.1) and (2.2) reads as: seek $(\mathbf{M}_h, \boldsymbol{\gamma}_h, w_h, \boldsymbol{\beta}_h) \in \mathbb{M}_h \times \Gamma_h \times W_h \times \Theta_h$ with

$$a(\mathbf{M}_h, \boldsymbol{\gamma}_h; \mathbf{Q}_h, \boldsymbol{\tau}_h) + b(\mathbf{Q}_h, \boldsymbol{\tau}_h; w_h, \boldsymbol{\beta}_h) = 0 \quad \text{for all } (\mathbf{Q}_h, \boldsymbol{\tau}_h) \in \mathbb{M}_h \times \Gamma_h, \quad (3.1)$$

$$b(\mathbf{M}_h, \boldsymbol{\gamma}_h; v_h, \zeta_h) = - \int_{\Omega} g v_h \, d\mathbf{x} \quad \text{for all } (v_h, \zeta_h) \in W_h \times \Theta_h. \quad (3.2)$$

Notice that in the continuous level the bending moment \mathbf{M} and the shear stress $\boldsymbol{\gamma}$ satisfy the equilibrium condition (1.2). To avoid ‘locking’ in the discretization problem (3.1) and (3.2), we assume (H1).

- (H1) The bending moment and shear stress approximation are coupled in the sense that

$$\Gamma_h = \mathbf{div}_h \mathbb{M}_h \quad (3.3)$$

and

$$(\mathbf{Q}_h, \boldsymbol{\tau}_h) := (\mathbf{Q}_h, \mathbf{div}_h \mathbf{Q}_h) \quad (3.4)$$

for $\mathbf{Q}_h \in \mathbb{M}_h$. Here \mathbf{div}_h denotes the divergence operator piecewise defined with respect to T_h .

Remark 3.1. With assumption (H1), we have an equivalent form of the discrete scheme (3.1) and (3.2): seek $(\mathbf{M}_h, w_h, \beta_h) \in \mathbb{M}_h \times W_h \times \Theta_h$ with

$$a(\mathbf{M}_h, \mathbf{div}_h \mathbf{M}_h; \mathbf{Q}_h, \mathbf{div}_h \mathbf{Q}_h) + b(\mathbf{Q}_h, \mathbf{div}_h \mathbf{Q}_h; w_h, \beta_h) = 0 \quad (3.5)$$

$$b(\mathbf{M}_h, \mathbf{div}_h \mathbf{M}_h; v_h, \zeta_h) = - \int_{\Omega} g v_h \, dx \quad \text{for all } (v_h, \zeta_h) \in W_h \times \Theta_h. \quad (3.6)$$

For the sake of convenience, we shall use the formulations (3.1) and (3.2) instead of (3.5) and (3.6) for the following discussion.

We introduce two mesh-dependent norms for the finite dimensional spaces $\mathbb{M}_h \times \Gamma_h$ and $W_h \times \Theta_h$: for $(\mathbf{Q}_h, \boldsymbol{\tau}_h) \in \mathbb{M}_h \times \Gamma_h$, $(v_h, \zeta_h) \in W_h \times \Theta_h$,

$$\|(\mathbf{Q}_h, \boldsymbol{\tau}_h)\|_{h,1}^2 := \|\mathbf{Q}_h\|_0^2 + (t^2 + h^2) \|\boldsymbol{\tau}_h\|_0^2, \quad (3.7)$$

$$\|(v_h, \zeta_h)\|_{h,2}^2 := \|\epsilon(\zeta_h)\|_0^2 + (t^2 + h^2)^{-1} \|\nabla v_h - \zeta_h\|_0^2. \quad (3.8)$$

Lemma 3.1. Under the assumption (H1), the discrete coercivity condition

$$\|(\mathbf{Q}_h, \boldsymbol{\tau}_h)\|_{h,1}^2 \lesssim a(\mathbf{Q}_h, \boldsymbol{\tau}_h; \mathbf{Q}_h, \boldsymbol{\tau}_h) \quad (3.9)$$

holds for all $(\mathbf{Q}_h, \boldsymbol{\tau}_h) \in \mathbb{M}_h \times \Gamma_h$.

Proof. We only need to show

$$h_K \|\boldsymbol{\tau}_h\|_{0,K} \lesssim \|\mathbf{Q}_h\|_{0,K} \quad \text{for all } (\mathbf{Q}_h, \boldsymbol{\tau}_h) \in \mathbb{M}_h \times \Gamma_h. \quad (3.10)$$

In fact, since $\boldsymbol{\tau}_h = \mathbf{div}_h \mathbf{Q}_h$, the above inequality follows from the inverse inequality, namely

$$\|\boldsymbol{\tau}_h\|_{0,K} = \|\mathbf{div}_h \mathbf{Q}_h\|_{0,K} \leq |\mathbf{Q}_h|_{1,K} \lesssim h^{-1} \|\mathbf{Q}_h\|_{0,K}. \quad \square$$

We further assume (H2) and (H3).

(H2) The energy-orthogonality condition

$$\int_K \boldsymbol{\tau}_h \cdot \nabla v_l \, dx = 0 \quad \text{for all } \boldsymbol{\tau}_h \in \Gamma_h, v_l \in B_h, K \in T_h \quad (3.11)$$

holds, where B_h is some bubble function space.

Remark 3.2. In fact, for B_h we will assume in (H5) that $W_h \oplus B_h$ has a higher order accuracy of approximation than the discrete transverse displacement space W_h , which is essential to the desired convergence order (cf. Theorem 3.2).

(H3) For all $(v_h, \zeta_h) \in W_h \times \Theta_h$, the following discrete inf-sup condition holds,

$$\|(v_h, \zeta_h)\|_{h,2} \lesssim \sup_{(\mathbf{Q}_h, \boldsymbol{\tau}_h) \in \mathbb{M}_h \times \Gamma_h} \frac{b(\mathbf{Q}_h, \boldsymbol{\tau}_h; v_h, \zeta_h)}{\|(\mathbf{Q}_h, \boldsymbol{\tau}_h)\|_{h,1}}. \quad (3.12)$$

Remark 3.3. With the norms defined in (3.7) and (3.8), the inf-sup condition

$$\|(v, \zeta)\|_{h,2} \leq \sup_{(\mathbf{Q}, \boldsymbol{\tau}) \in \mathbb{M} \times \Gamma} \frac{b(\mathbf{Q}, \boldsymbol{\tau}; v, \zeta)}{\|(\mathbf{Q}, \boldsymbol{\tau})\|_{h,1}} \quad (3.13)$$

immediately follows for all $(v, \zeta) \in W \times \Theta$.

We now state the first main result of this section.

Theorem 3.1. Assume the conditions (H1)–(H3) hold. Let $(\mathbf{M}, \boldsymbol{\gamma}, w, \beta) \in \mathbb{M} \times \Gamma \times W \times \Theta$ be the solution of the problem (2.1) and (2.2). Then the discretization problem (3.1) and (3.2) admits a unique solution $(\mathbf{M}_h, \boldsymbol{\gamma}_h = \mathbf{div}_h \mathbf{M}_h, w_h, \beta_h) \in \mathbb{M}_h \times \Gamma_h \times W_h \times \Theta_h$ such that

$$\|\mathbf{M} - \mathbf{M}_h\|_0 + (h+t) \|\boldsymbol{\gamma} - \boldsymbol{\gamma}_h\|_0 \lesssim \inf_{(\mathbf{Q}_h, \boldsymbol{\tau}_h) \in \mathbb{M}_h \times \Gamma_h} (\|\mathbf{M} - \mathbf{Q}_h\|_0 + (h+t) \|\boldsymbol{\gamma} - \boldsymbol{\tau}_h\|_0) + \inf_{\zeta_h \in \Theta_h} (\|\epsilon(\beta - \zeta_h)\|_0 + h^{-1} \|\beta - \zeta_h\|_0) + \inf_{v_h + v_l \in W_h \oplus B_h} h^{-1} \|\nabla(w - v_h - v_l)\|_0, \quad (3.14)$$

$$\|\epsilon(\beta - \beta_h)\|_0 \lesssim \|\mathbf{M} - \mathbf{M}_h\|_0 + t \|\boldsymbol{\gamma} - \boldsymbol{\gamma}_h\|_0 + \inf_{\zeta_h \in \Theta_h} (\|\epsilon(\beta - \zeta_h)\|_0 + h^{-1} \|\beta - \zeta_h\|_0) + \inf_{v_h + v_l \in W_h \oplus B_h} h^{-1} \|\nabla(w - v_h - v_l)\|_0, \quad (3.15)$$

$$\|\nabla(w - w_h) - (\beta - \beta_h)\|_0 \lesssim (h+t) \|\mathbf{M} - \mathbf{M}_h\|_0 + t^2 \|\boldsymbol{\gamma} - \boldsymbol{\gamma}_h\|_0 + \inf_{\zeta_h \in \Theta_h} (\|\epsilon(\beta - \zeta_h)\|_0 + \|\beta - \zeta_h\|_0) + \inf_{v_h \in W_h} \|\nabla(w - v_h)\|_0. \quad (3.16)$$

Proof. Existence of the discrete solution $(\mathbf{M}_h, \boldsymbol{\gamma}_h, w_h, \beta_h)$ is easy. The estimates (3.14)–(3.16) follow from a standard line as in [14,18], except that the energy orthogonality relation (3.11) is included in the analysis. For completeness we sketch the proof.

Subtracting Eq. (3.1) from (2.1), we have for all $(\mathbf{Q}_h, \boldsymbol{\tau}_h) \in \mathbb{M}_h \times \Gamma_h$,

$$a(\mathbf{M} - \mathbf{M}_h, \boldsymbol{\gamma} - \boldsymbol{\gamma}_h; \mathbf{Q}_h, \boldsymbol{\tau}_h) + b(\mathbf{Q}_h, \boldsymbol{\tau}_h; w - w_h, \beta - \beta_h) = 0. \quad (3.17)$$

Denote

$$\mathbf{Z}_h(\mathbf{g}) := \left\{ (\mathbf{Q}_h, \boldsymbol{\tau}_h) \in \mathbb{M}_h \times \Gamma_h : b(\mathbf{Q}_h, \boldsymbol{\tau}_h; v_h, \zeta_h) = - \int_{\Omega} g v_h \, dx \quad \text{for all } (v_h, \zeta_h) \in W_h \times \Theta_h \right\}.$$

Due to the discrete inf-sup condition (3.12) and Remark 3.3, by Proposition II-2.5 in [18] (Chapter II, p. 55), we obtain

$$\inf_{(\mathbf{Q}_h, \boldsymbol{\tau}_h) \in \mathbf{Z}_h(\mathbf{g})} \|(\mathbf{M} - \mathbf{Q}_h, \boldsymbol{\gamma} - \boldsymbol{\tau}_h)\|_{h,1} \lesssim \inf_{(\mathbf{Q}_h, \boldsymbol{\tau}_h) \in \mathbb{M}_h \times \Gamma_h} \|(\mathbf{M} - \mathbf{Q}_h, \boldsymbol{\gamma} - \boldsymbol{\tau}_h)\|_{h,1}. \quad (3.18)$$

Taking $(\mathbf{Q}_h, \boldsymbol{\tau}_h) = (\tilde{\mathbf{Q}}_h - \mathbf{M}_h, \tilde{\boldsymbol{\tau}}_h - \boldsymbol{\gamma}_h)$ in (3.17) with $(\tilde{\mathbf{Q}}_h, \tilde{\boldsymbol{\tau}}_h) \in \mathbf{Z}_h(\mathbf{g})$, from Lemma 3.1 we deduce

$$\begin{aligned} \|(\tilde{\mathbf{Q}}_h - \mathbf{M}_h, \tilde{\boldsymbol{\tau}}_h - \boldsymbol{\gamma}_h)\|_{h,1}^2 &\lesssim a(\tilde{\mathbf{Q}}_h - \mathbf{M}_h, \tilde{\boldsymbol{\tau}}_h - \boldsymbol{\gamma}_h; \tilde{\mathbf{Q}}_h - \mathbf{M}_h, \tilde{\boldsymbol{\tau}}_h - \boldsymbol{\gamma}_h) \\ &+ a(\mathbf{M} - \tilde{\mathbf{Q}}_h, \boldsymbol{\gamma} - \tilde{\boldsymbol{\tau}}_h; \tilde{\mathbf{Q}}_h - \mathbf{M}_h, \tilde{\boldsymbol{\tau}}_h - \boldsymbol{\gamma}_h) \\ &= a(\tilde{\mathbf{Q}}_h - \mathbf{M}_h, \tilde{\boldsymbol{\tau}}_h - \boldsymbol{\gamma}_h; \tilde{\mathbf{Q}}_h - \mathbf{M}_h, \tilde{\boldsymbol{\tau}}_h - \boldsymbol{\gamma}_h) \\ &\quad - b(\tilde{\mathbf{Q}}_h - \mathbf{M}_h, \tilde{\boldsymbol{\tau}}_h - \boldsymbol{\gamma}_h; w - w_h, \beta - \beta_h) \\ &= a(\tilde{\mathbf{Q}}_h - \mathbf{M}_h, \tilde{\boldsymbol{\tau}}_h - \boldsymbol{\gamma}_h; \tilde{\mathbf{Q}}_h - \mathbf{M}_h, \tilde{\boldsymbol{\tau}}_h - \boldsymbol{\gamma}_h) \\ &\quad - b(\tilde{\mathbf{Q}}_h - \mathbf{M}_h, \tilde{\boldsymbol{\tau}}_h - \boldsymbol{\gamma}_h; w - v_h - v_l, \beta - \zeta_h), \end{aligned}$$

where $(v_h, v_l, \zeta_h) \in W_h \times B_h \times \Theta_h$, and in the last equality we have used the fact $(\tilde{\mathbf{Q}}_h, \tilde{\boldsymbol{\tau}}_h) \in \mathbf{Z}_h(\mathbf{g})$ and the relation

$$b(\mathbf{Q}_h, \boldsymbol{\tau}_h; v_l, 0) = \sum_K \int_K \boldsymbol{\tau}_h \cdot \nabla v_l = 0 \quad \text{for all } (\mathbf{Q}_h, \boldsymbol{\tau}_h) \in \mathbb{M}_h \times \Gamma_h, v_l \in B_h$$

which is inferred from the assumption (H2). A combination of the above inequality, Cauchy-schwarz inequality and arbitrariness of the triple (v_h, v_l, ζ_h) yields

$$\begin{aligned} \|(\tilde{\mathbf{Q}}_h - \mathbf{M}_h, \tilde{\boldsymbol{\tau}}_h - \boldsymbol{\gamma}_h)\|_{h,1} &\lesssim \|(\tilde{\mathbf{Q}}_h - \mathbf{M}_h, \tilde{\boldsymbol{\tau}}_h - \boldsymbol{\gamma}_h)\|_{h,1} + \inf_{\zeta_h \in \Theta_h} (\|\epsilon(\beta - \zeta_h)\|_0 \\ &+ (h+t)^{-1} \|\beta - \zeta_h\|_0) + \inf_{v_h + v_l \in W_h \oplus B_h} (h+t)^{-1} \|\nabla(w - v_h - v_l)\|_0. \end{aligned}$$

Then the estimate (3.14) follows from triangle inequality, arbitrariness of $(\tilde{\mathbf{Q}}_h, \tilde{\boldsymbol{\tau}}_h) \in \mathbf{Z}_h(\mathbf{g})$ and the conclusion (3.18).

Next we estimate $\|\epsilon(\beta - \beta_h)\|_0$ and $\|\nabla(w - w_h) - (\beta - \beta_h)\|_0$. The discrete inf-sup inequality (3.12), together with Eq. (3.17) and the assumption (H2), indicates, for any $(v_h, v_l, \zeta) \in W_h \times B_h \times \Theta_h$,

$$\begin{aligned} \|(v_h - w_h, \zeta_h - \beta_h)\|_{h,2} &\lesssim \sup_{(\mathbf{Q}_h, \boldsymbol{\tau}_h) \in \mathbb{M}_h \times \Gamma_h} \frac{b(\mathbf{Q}_h, \boldsymbol{\tau}_h; v_h - w_h, \zeta_h - \beta_h)}{\|(\mathbf{Q}_h, \boldsymbol{\tau}_h)\|_{h,1}} \\ &= \sup_{(\mathbf{Q}_h, \boldsymbol{\tau}_h) \in \mathbb{M}_h \times \Gamma_h} \frac{-a(\mathbf{M} - \mathbf{M}_h, \boldsymbol{\gamma} - \boldsymbol{\gamma}_h; \mathbf{Q}_h, \boldsymbol{\tau}_h) - b(\mathbf{Q}_h, \boldsymbol{\tau}_h; w - v_l, \beta - \zeta_h)}{\|(\mathbf{Q}_h, \boldsymbol{\tau}_h)\|_{h,1}} \\ &\lesssim \|\mathbf{M} - \mathbf{M}_h\|_0 + \|\epsilon(\beta - \zeta_h)\|_0 \\ &\quad + \sup_{\boldsymbol{\tau}_h \in \Gamma_h} \frac{\int_{\Omega} (\boldsymbol{\gamma} - \boldsymbol{\gamma}_h) \cdot \boldsymbol{\tau}_h \, d\mathbf{x} - \int_{\Omega} \boldsymbol{\tau}_h \cdot (\nabla(w - v_l) - (\beta - \zeta_h)) \, d\mathbf{x}}{(h+t)\|\boldsymbol{\tau}_h\|_0} \\ &\lesssim \|\mathbf{M} - \mathbf{M}_h\|_0 + \|\epsilon(\beta - \zeta_h)\|_0 + (h+t)^{-1} (t^2 \|\boldsymbol{\gamma} - \boldsymbol{\gamma}_h\|_0 + \|\beta - \zeta_h\|_0 \\ &\quad + \|\nabla(w - v_l)\|_0). \end{aligned}$$

The desired estimates (3.15) and (3.16) then follow from the above inequality, triangle inequality and arbitrariness of $(v_h, v_l, \zeta_h) \in W_h \times B_h \times \Theta_h$. \square

We assume the following approximation results (H4)–(H5) hold for the finite dimensional spaces $\mathbb{M}_h \times \Gamma_h, W_h, B_h$ and Θ_h .

(H4) Suppose that

$$\inf_{(\mathbf{Q}_h, \boldsymbol{\tau}_h) \in \mathbb{M}_h \times \Gamma_h} (\|\mathbf{Q}_h - \mathbf{M}\|_0 + (h+t)\|\boldsymbol{\tau}_h - \boldsymbol{\gamma}\|_0) \lesssim h(\|\mathbf{M}\|_1 + \|\boldsymbol{\gamma}\|_0 + t\|\boldsymbol{\gamma}\|_1); \quad (3.19)$$

(H5) Suppose that

$$\inf_{v_h \in W_h} \|\nabla(w - v_h)\|_0 \lesssim h\|w\|_2, \quad (3.20)$$

$$\inf_{v_h + v_l \in W_h \oplus B_h} \|\nabla(w - v_h - v_l)\|_0 \lesssim h^2\|w\|_3, \quad (3.21)$$

$$\inf_{\zeta_h \in \Theta_h} (\|\beta - \zeta_h\|_0 + h\|\beta - \zeta_h\|_1) \lesssim h^2\|\beta\|_2. \quad (3.22)$$

Remark 3.4. Recall that $\boldsymbol{\tau}_h = \text{div}_h \mathbf{Q}_h$, $\boldsymbol{\gamma} = \text{div} \mathbf{M}$. When $t \lesssim h$, (H4) can be simplified as

$$\inf_{\mathbf{Q}_h \in \mathbb{M}_h} (\|\mathbf{Q}_h - \mathbf{M}\|_0 + h\|\text{div}_h(\mathbf{Q}_h - \mathbf{M})\|_0) \lesssim h(\|\mathbf{M}\|_1 + t\|\text{div} \mathbf{M}\|_1).$$

As a result, from Theorem (3.1) we have the following uniform a priori results.

Theorem 3.2. Under the assumptions (H1)–(H5), the discretization problem (3.1) and (3.2) admits a unique solution $(\mathbf{M}_h, \boldsymbol{\gamma}_h = \text{div}_h \mathbf{M}_h, w_h, \beta_h) \in \mathbb{M}_h \times \Gamma_h \times W_h \times \Theta_h$ such that

$$\|\mathbf{M} - \mathbf{M}_h\|_0 + (h+t)\|\boldsymbol{\gamma} - \boldsymbol{\gamma}_h\|_0 + \|\beta - \beta_h\|_1 + \|w - w_h\|_1 \lesssim h(\|\mathbf{M}\|_1 + t\|\boldsymbol{\gamma}\|_1 + \|\boldsymbol{\gamma}\|_0 + \|\beta\|_2 + \|w\|_3). \quad (3.23)$$

Proof. The desired estimate follows from the estimates (3.14)–(3.16), the approximation properties (3.19)–(3.22), and equivalence between the norms $\|\nabla \cdot\|_0$ and $\|\cdot\|_1$ on $H_0^1(\Omega)$ due to Poincaré inequality and equivalence between the norms $\|\epsilon(\cdot)\|_0$ and $\|\cdot\|_1$ on $H_0^1(\Omega)^2$ due to Korn’s inequality. \square

In the final part of this section, we shall propose a sufficient condition for the approximation assumption (H4). We state the following assumption.

(H4’) Suppose there exists $\mathbb{M}_0^h \subset \mathbb{M}_h$ with

$$\text{div}_h \mathbf{Q}_h = 0 \quad \text{for all } \mathbf{Q}_h \in \mathbb{M}_0^h \quad (3.24)$$

and

$$\inf_{\mathbf{Q}_h \in \mathbb{M}_0^h} \|\mathbf{Q}_h - \mathbf{M}\|_0 \lesssim h\|\mathbf{M}\|_1. \quad (3.25)$$

Lemma 3.2. If the plate is sufficiently thin,

$$t \lesssim h, \quad (3.26)$$

then assumptions (H1) and (H4’) imply (H4).

Proof. Since $\mathbb{M}_0^h \times \{0\} \subset \mathbb{M}_h \times \Gamma_h$, from the approximation result (3.25) and the condition (3.26) we immediately have

$$\begin{aligned} &\inf_{(\mathbf{Q}_h, \boldsymbol{\tau}_h) \in \mathbb{M}_h \times \Gamma_h} (\|\mathbf{Q}_h - \mathbf{M}\|_0 + (h+t)\|\boldsymbol{\tau}_h - \boldsymbol{\gamma}\|_0) \\ &\leq \inf_{\mathbf{Q}_h \in \mathbb{M}_0^h} \|\mathbf{Q}_h - \mathbf{M}\|_0 + (h+t)\|\boldsymbol{\gamma}\|_0 \lesssim h(\|\mathbf{M}\|_1 + \|\boldsymbol{\gamma}\|_0). \quad \square \end{aligned}$$

Remark 3.5. In fact, one can avoid the numerical thinness condition (3.26) by using a more complicated space \mathbb{M}_h . Namely, \mathbb{M}_h is such that there exists $\boldsymbol{\tau}_h \mathbf{M} \in \mathbb{M}_h$ with

$$\|\boldsymbol{\tau}_h \mathbf{M} - \mathbf{M}\|_0 \lesssim h\|\mathbf{M}\|_1, \quad \|\text{div}_h(\boldsymbol{\tau}_h \mathbf{M} - \mathbf{M})\|_0 \lesssim h\|\text{div} \mathbf{M}\|_1. \quad (3.27)$$

Then (H4) follows from assumption (H1).

4. Construction of locking-free quadrilateral FEMs

4.1. Geometric properties of quadrilaterals

Let T_h be a conventional quadrilateral mesh of Ω . We denote by h_K the diameter of a quadrilateral $K \in T_h$, and denote $h := \max_{K \in T_h} h_K$. Let $Z_i(x_i, y_i)$, $1 \leq i \leq 4$ be the four vertices of K , and T_i be the sub-triangle of K with vertices Z_{i-1} , Z_i and Z_{i+1} (the index on Z_i is modulo 4). Define

$$\rho_K = \min_{1 \leq i \leq 4} \{\text{diameter of circle inscribed in } T_i\}.$$

Throughout the paper, we assume that the partition T_h satisfies the following shape-regularity hypothesis: there exists a constant $\varrho > 2$ independent of h such that for all $K \in T_h$,

$$h_K \leq \varrho \rho_K. \quad (4.1)$$

Remark 4.1. As shown in [33], this shape regularity condition is equivalent to the following one which has been widely used in literature (e.g. [23]): there exist two constants $\varrho' > 2$ and $0 < \gamma < 1$ independent of h such that for all $K \in T_h$,

$$h_K \leq \varrho' \rho'_K, \quad |\cos \theta_K^i| \leq \gamma, \quad 1 \leq i \leq 4, \quad (4.2)$$

where ρ'_K and θ_K^i denote the maximum diameter of all circles contained in K and the angles associated with vertices of K , respectively.

Let $\hat{K} = [-1, 1] \times [-1, 1]$ be the reference square with vertices \hat{Z}_i ($1 \leq i \leq 4$). There exists a unique invertible mapping F_K that maps \hat{K} onto K with $F_K(\xi, \eta) \in P_{1,1}^2(\xi, \eta)$ and $F_K(\hat{Z}_i) = Z_i$, $1 \leq i \leq 4$ (Fig. 1). Here $\xi, \eta \in [-1, 1]$ are the local isoparametric coordinates.

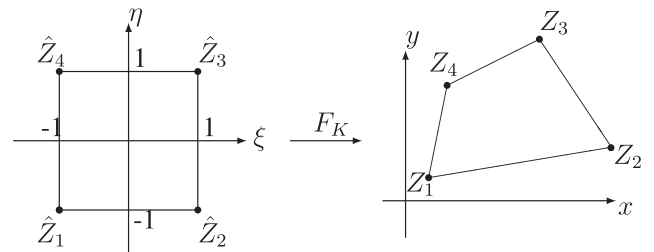


Fig. 1. The mapping F_K .

This isoparametric bilinear mapping $(x, y) = F_K(\xi, \eta)$ is given by

$$x = \sum_{i=1}^4 x_i N_i(\xi, \eta), y = \sum_{i=1}^4 y_i N_i(\xi, \eta), \tag{4.3}$$

where

$$N_1 = \frac{1}{4}(1 - \xi)(1 - \eta), \quad N_2 = \frac{1}{4}(1 + \xi)(1 - \eta), \\ N_3 = \frac{1}{4}(1 + \xi)(1 + \eta), \quad N_4 = \frac{1}{4}(1 - \xi)(1 + \eta).$$

We can rewrite (4.3) as

$$x = a_0 + a_1 \xi + a_2 \eta + a_{12} \xi \eta, \quad y = b_0 + b_1 \xi + b_2 \eta + b_{12} \xi \eta, \tag{4.4}$$

where

$$\begin{pmatrix} a_0 & b_0 \\ a_1 & b_1 \\ a_2 & b_2 \\ a_{12} & b_{12} \end{pmatrix} = \frac{1}{4} \begin{pmatrix} 1 & 1 & 1 & 1 \\ -1 & 1 & 1 & -1 \\ -1 & -1 & 1 & 1 \\ 1 & -1 & 1 & -1 \end{pmatrix} \begin{pmatrix} x_1 & y_1 \\ x_2 & y_2 \\ x_3 & y_3 \\ x_4 & y_4 \end{pmatrix}.$$

The Jacobi matrix of the transformation F_K is

$$DF_K(\xi, \eta) = \begin{pmatrix} \frac{\partial x}{\partial \xi} & \frac{\partial x}{\partial \eta} \\ \frac{\partial y}{\partial \xi} & \frac{\partial y}{\partial \eta} \end{pmatrix} = \begin{pmatrix} a_1 + a_{12} \eta & a_2 + a_{12} \xi \\ b_1 + b_{12} \eta & b_2 + b_{12} \xi \end{pmatrix},$$

and the Jacobian of F_K equals

$$J_K = \det(DF_K) = J_0 + J_1 \xi + J_2 \eta,$$

where

$$J_0 = a_1 b_2 - a_2 b_1, \quad J_1 = a_1 b_{12} - a_{12} b_1, \quad J_2 = a_{12} b_2 - a_2 b_{12}.$$

Denote by F_K^{-1} the inverse of F_K . Then we compute

$$\begin{pmatrix} \frac{\partial \xi}{\partial x} & \frac{\partial \xi}{\partial y} \\ \frac{\partial \eta}{\partial x} & \frac{\partial \eta}{\partial y} \end{pmatrix} = \frac{1}{J_K} \begin{pmatrix} b_2 + b_{12} \xi & -a_2 - a_{12} \xi \\ -b_1 - b_{12} \eta & a_1 + a_{12} \eta \end{pmatrix}.$$

Remark 4.2. Notice that $a_{12} = b_{12} = 0$ and F_K is an affine mapping when K is a parallelogram. Especially, when K is a rectangle, $a_2 = b_1 = 0$.

Let the midpoint of edge $Z_i Z_{i+1}$ be M_i for $i = 1, \dots, 4$, and let the midpoints of $Z_2 Z_4, Z_1 Z_3$ be O_1, O_2 , respectively. It is easy to verify that

$$M_4 M_2 = (x_{M_2} - x_{M_4}, y_{M_2} - y_{M_4}) = 2(a_1, b_1), \tag{4.5}$$

$$M_1 M_3 = (x_{M_3} - x_{M_1}, y_{M_3} - y_{M_1}) = 2(a_2, b_2), \tag{4.6}$$

$$O_1 O_2 = (x_{O_2} - x_{O_1}, y_{O_2} - y_{O_1}) = 2(a_{12}, b_{12}). \tag{4.7}$$

Then it follows

$$2\sqrt{a_1^2 + b_1^2} = |M_4 M_2|, \quad 2\sqrt{a_2^2 + b_2^2} = |M_1 M_3|, \quad 2\sqrt{a_{12}^2 + b_{12}^2} = |O_1 O_2|. \tag{4.8}$$

It holds the following element geometric properties.

Lemma 4.1 (See [45]). For any $K \in T_h$, under the hypothesis (4.1), we have

$$\frac{\max_{(\xi, \eta) \in \hat{K}} J_K}{\min_{(\xi, \eta) \in \hat{K}} J_K} < \frac{h_K^2}{2\rho_K^2} \leq \frac{\rho^2}{2}, \tag{4.9}$$

$$\frac{1}{4} \rho_K^2 < a_1^2 + b_1^2 < \frac{1}{4} h_K^2, \quad \frac{1}{4} \rho_K^2 < a_2^2 + b_2^2 < \frac{1}{4} h_K^2, \tag{4.10}$$

$$a_{12}^2 + b_{12}^2 < \frac{1}{16} h_K^2. \tag{4.11}$$

In view of the choice of node order (cf. Fig. 1), the shape-regular hypothesis (4.1) and the relations (4.5) and (4.6), without loss of generality we assume

$$|b_1| \leq a_1, \quad |a_2| \leq b_2. \tag{4.12}$$

Together with (4.10), this leads to

$$a_1 \approx b_2 \approx h_K, \quad \max\{a_2, b_1\} = O(h_K). \tag{4.13}$$

Notice also that (4.9) implies

$$J_K \approx J_0 \approx h_K^2. \tag{4.14}$$

4.2. Construction of finite element subspaces

In this subsection, we will construct the spaces $\mathbb{M}_h, \Gamma_h, W_h$ and Θ_h on quadrilateral meshes in accordance with the assumptions (H1)–(H5).

For the transverse displacement and rotation approximation we use continuous isoparametric bilinear element, i.e. we take

$$W_h := \left\{ v_h \in H_0^1(\Omega) \cap C(\bar{\Omega}) : \hat{v} = v_h|_K \circ F_K \in P_{1,1}(\hat{K}) \text{ for all } K \in T_h \right\}, \tag{4.15}$$

$$\Theta_h := \left\{ \zeta_h \in (H_0^1(\Omega) \cap C(\bar{\Omega}))^2 : \hat{\zeta} = \zeta_h|_K \circ F_K \in P_{1,1}(\hat{K})^2 \text{ for all } K \in T_h \right\}. \tag{4.16}$$

Let B_h be the Wilson bubble function space defined as

$$B_h := \left\{ v_l \in L^2(\Omega) : \hat{v}_l = v_l|_K \circ F_K \in \text{span}\{1 - \xi^2, 1 - \eta^2\} \text{ for all } K \in T_h \right\}. \tag{4.17}$$

Introduce the modified local coordinates $\bar{\xi}, \bar{\eta}$ as in [43] by

$$\begin{Bmatrix} \bar{\xi} \\ \bar{\eta} \end{Bmatrix} := \frac{1}{J_0} \begin{Bmatrix} b_2 x - a_2 y - a_0 b_2 + a_2 b_0 \\ -b_1 x + a_1 y + a_0 b_1 - a_1 b_0 \end{Bmatrix} = \begin{Bmatrix} \xi + \frac{a_{12} b_2 - a_2 b_{12}}{J_0} \xi \eta \\ \eta + \frac{a_{12} b_1 - a_1 b_{12}}{J_0} \xi \eta \end{Bmatrix}. \tag{4.18}$$

It is easy to see that

$$\begin{Bmatrix} x \\ y \end{Bmatrix} = \begin{Bmatrix} a_0 + a_1 \bar{\xi} + a_2 \bar{\eta} \\ b_0 + b_1 \bar{\xi} + b_2 \bar{\eta} \end{Bmatrix}. \tag{4.19}$$

We define

$$\Gamma_h := \left\{ \tau_h \in L^2(\Omega)^2 : \hat{\tau} = \tau_h|_K \circ F_K \in \text{span}\{1, \bar{\xi}, \bar{\eta}\}^2 \text{ and } \int_K \tau_h \cdot \nabla v_l d\mathbf{x} = 0 \text{ for all } v_l \in B_h, K \in T_h \right\}. \tag{4.20}$$

Some calculations show that, for any $\tau_h \in \Gamma_h$, $\hat{\tau} = \tau_h|_K \circ F_K$ has the form

$$\hat{\tau} = \begin{pmatrix} 1 - \frac{b_{12}}{b_2} \bar{\xi} & \frac{a_{12}}{b_2} \bar{\xi} & \bar{\eta} & \frac{a_2}{b_2} \bar{\xi} \\ \frac{b_{12}}{a_1} \bar{\eta} & 1 - \frac{a_{12}}{a_1} \bar{\eta} & \frac{b_1}{a_1} \bar{\eta} & \bar{\xi} \end{pmatrix} \begin{pmatrix} \bar{c}_1 \\ \vdots \\ \bar{c}_4 \end{pmatrix} =: \Phi_s \begin{pmatrix} \bar{c}_1 \\ \vdots \\ \bar{c}_4 \end{pmatrix} \text{ for all } \bar{c}_i \in \mathbb{R}. \tag{4.21}$$

Thus, the assumption (H2) is fulfilled for Γ_h .

Remark 4.3. It is easy to see that $\text{div}_h \tau_h|_K = 0$ holds for $\tau_h \in \Gamma_h$.

Remark 4.4. When K is a rectangle, the stress form (4.21) is reduced to

$$\hat{\tau} = \begin{bmatrix} 1 & 0 & \eta & 0 \\ 0 & 1 & 0 & \xi \end{bmatrix} \begin{Bmatrix} \bar{c}_1 \\ \vdots \\ \bar{c}_4 \end{Bmatrix}. \tag{4.22}$$

For the approximation of bending moment tensor, we define

$$\mathbb{M}_h := \mathbb{M}_0^h \oplus \mathbb{M}_1^h \quad (4.23)$$

with

$$\mathbb{M}_0^h := \left\{ \mathbf{Q}_h \in L^2(\Omega)_{\text{sym}}^{2 \times 2} : \widehat{\mathbf{Q}} = \mathbf{Q}_h|_K \circ F_K \text{ is of the form (4.25)} \right. \\ \left. \text{for all } K \in T_h, \quad i, j = 1, 2 \right\}, \quad (4.24)$$

$$\widehat{\mathbf{Q}} = \begin{pmatrix} \widehat{Q}_{11} \\ \widehat{Q}_{22} \\ \widehat{Q}_{12} \end{pmatrix} = \begin{pmatrix} 1 & 0 & 0 & \bar{\eta} & \frac{a_2^2}{b_2^2} \bar{\xi} \\ 0 & 1 & 0 & \frac{b_1^2}{a_1^2} \bar{\eta} & \bar{\xi} \\ 0 & 0 & 1 & \frac{b_1}{a_1} \bar{\eta} & \frac{a_2}{b_2} \bar{\xi} \end{pmatrix} \begin{pmatrix} c_1 \\ \vdots \\ c_5 \end{pmatrix} =: \Phi_0 \begin{pmatrix} c_1 \\ \vdots \\ c_5 \end{pmatrix} \\ \text{for all } c_i \in \mathbb{R}. \quad (4.25)$$

The finite-dimensional space \mathbb{M}_1^h will be defined such that

$$\mathbb{M}_1^h \cap \mathbb{M}_0^h = \{0\} \text{ and } \mathbf{div}_h \mathbb{M}_1^h = \Gamma_h. \quad (4.26)$$

Here and in the sequel, we use the Voigt notation $\mathbf{Q} = (Q_{11}, Q_{22}, Q_{12})^T$ to denote a symmetric tensor $\mathbf{Q} = \begin{pmatrix} Q_{11} & Q_{12} \\ Q_{12} & Q_{22} \end{pmatrix}$ for the sake of convenience.

Remark 4.5. In the following we also simplify a strain tensor $\epsilon(\zeta) = \frac{1}{2}(\nabla + \nabla^T)\zeta$ as $\epsilon(\zeta) = \left(\frac{\partial \zeta^{(1)}}{\partial x}, \frac{\partial \zeta^{(2)}}{\partial y}, \frac{\partial \zeta^{(1)}}{\partial y} + \frac{\partial \zeta^{(2)}}{\partial x} \right)^T$. Then, for a symmetric moment tensor $\mathbf{Q} = (Q_{ij})_{2 \times 2}$ we have

$$\mathbf{Q} : \epsilon(\zeta) = \mathbf{Q} \cdot \epsilon(\zeta) = (Q_{11}, Q_{22}, Q_{12}) \begin{pmatrix} \frac{\partial \zeta^{(1)}}{\partial x} \\ \frac{\partial \zeta^{(2)}}{\partial y} \\ \frac{\partial \zeta^{(1)}}{\partial y} + \frac{\partial \zeta^{(2)}}{\partial x} \end{pmatrix}.$$

It is easy to verify

$$\mathbf{div}_h \mathbf{Q}_h|_K = 0 \quad \text{for all } \mathbf{Q}_h \in \mathbb{M}_0^h. \quad (4.27)$$

Then from (4.26) it follows

$$\mathbf{div}_h \mathbf{Q}_h \mathbb{M}_h = \Gamma_h. \quad (4.28)$$

Remark 4.6. Similar to [42,43,48], we can rewrite the subspace \mathbb{M}_0^h in an equivalent form, namely

$$\mathbb{M}_0^h = \left\{ \mathbf{Q}_h \in L^2(\Omega)_{\text{sym}}^{2 \times 2} : \widehat{\mathbf{Q}} = \mathbf{Q}_h|_K \circ F_K \in \text{span}\{1, \bar{\xi}, \bar{\eta}\}_{\text{sym}}^{2 \times 2}, \quad i, j = 1, 2 \right. \\ \left. \text{and } \int_K (\mathbf{Q}_h - \mathbf{Q}_{h,c}) : \epsilon(\zeta_l) \, d\mathbf{x} = 0 \text{ for all } \zeta_l \in (B_h)^2, \quad K \in T_h \right\}$$

with $\mathbf{Q}_{h,c}$ being the constant part of \mathbf{Q}_h .

Remark 4.7. One can also choose a larger space

$$\mathbb{M}_{01}^h := \{ \mathbf{Q}_h \in L^2(\Omega)_{\text{sym}}^{2 \times 2} : \widehat{\mathbf{Q}} = \mathbf{Q}_h|_K \circ F_K \\ \in \text{span}\{1, \bar{\xi}, \bar{\eta}\} \text{ and } \mathbf{div}_h \mathbf{Q}_h|_K = 0 \text{ for all } K \in T_h, \quad i, j = 1, 2 \},$$

to replace \mathbb{M}_0^h , where $\widehat{\mathbf{Q}} = \mathbf{Q}_h|_K \circ F_K$ has the form

$$\widehat{\mathbf{Q}} = \begin{pmatrix} \widehat{Q}_{11} \\ \widehat{Q}_{22} \\ \widehat{Q}_{12} \end{pmatrix} = \begin{pmatrix} 1 & 0 & 0 & \bar{\xi} & \bar{\eta} & 0 & 0 \\ 0 & 1 & 0 & 0 & 0 & \bar{\xi} & \bar{\eta} \\ 0 & 0 & 1 & -b_2 f_1 & b_1 f_1 & a_2 f_2 & -a_1 f_2 \end{pmatrix} \begin{pmatrix} c_1 \\ \vdots \\ c_7 \end{pmatrix}$$

with $f_1 := \frac{1}{j_0}(b_1 \bar{\xi} + b_2 \bar{\eta})$, $f_2 := \frac{1}{j_0}(a_1 \bar{\xi} + a_2 \bar{\eta})$, and $c_i \in \mathbb{R}$. However, some numerical results show that the choice of \mathbb{M}_{01}^h cannot lead to better stability or accuracy than the choice of \mathbb{M}_0^h .

The construction of \mathbb{M}_0^h and \mathbb{M}_1^h in (4.23) is, on the one hand, to satisfy the relation (4.28); on the other hand, as far as analysis is concerned, it should be made convenient for verifying the discrete inf-sup condition (3.12). To this end, for $\zeta_h \in \Theta_h$ we denote

$$\zeta_h|_K := \zeta_1 + \zeta_2 = (\hat{\zeta}_1 + \hat{\zeta}_2) \circ F_K^{-1} \quad (4.29)$$

with

$$\hat{\zeta}_1 := \begin{pmatrix} \bar{\zeta}_7 - \frac{1}{j_0}(b_1 \bar{\xi} + b_2 \bar{\eta} + b_{12} \bar{\xi} \bar{\eta}) \bar{\zeta}_6 \\ \bar{\zeta}_8 + \frac{1}{j_0}(a_1 \bar{\xi} + a_2 \bar{\eta} + a_{12} \bar{\xi} \bar{\eta}) \bar{\zeta}_6 \end{pmatrix}, \quad (4.30)$$

$$\hat{\zeta}_2 = \begin{pmatrix} \bar{\zeta}_2^{(1)} \\ \bar{\zeta}_2^{(2)} \end{pmatrix} := \begin{pmatrix} \bar{\xi} & \bar{\eta} & \bar{\xi} \bar{\eta} & 0 & 0 \\ 0 & 0 & 0 & \bar{\eta} & \bar{\xi} \bar{\eta} \end{pmatrix} \begin{pmatrix} \bar{\zeta}_1 \\ \vdots \\ \bar{\zeta}_5 \end{pmatrix} =: \Phi_r \begin{pmatrix} \bar{\zeta}_1 \\ \vdots \\ \bar{\zeta}_5 \end{pmatrix} \quad (4.31)$$

for any $\bar{\zeta}_i \in \mathbb{R}$. Then it follows $\epsilon(\zeta_1) = 0$ and

$$\epsilon(\zeta_h)|_K = \epsilon(\zeta_2) := \begin{pmatrix} \frac{\partial \zeta_2^{(1)}}{\partial x} \\ \frac{\partial \zeta_2^{(2)}}{\partial y} \\ \frac{\partial \zeta_2^{(1)}}{\partial y} + \frac{\partial \zeta_2^{(2)}}{\partial x} \end{pmatrix} = B \begin{pmatrix} \bar{\zeta}_1 \\ \vdots \\ \bar{\zeta}_5 \end{pmatrix} \quad (4.32)$$

with

$$B = \frac{1}{j_K} \begin{pmatrix} b_2 + b_{12} \bar{\xi} & -b_1 - b_{12} \bar{\eta} & -b_1 \bar{\xi} + b_2 \bar{\eta} & 0 & 0 \\ 0 & 0 & 0 & a_1 + a_{12} \bar{\eta} & a_1 \bar{\xi} - a_2 \bar{\eta} \\ -a_2 - a_{12} \bar{\xi} & a_1 + a_{12} \bar{\eta} & a_1 \bar{\xi} - a_2 \bar{\eta} & -b_1 - b_{12} \bar{\eta} & -b_1 \bar{\xi} + b_2 \bar{\eta} \end{pmatrix}.$$

Besides (4.26), we shall enhance a constraint on \mathbb{M}_1^h , namely for all $\mathbf{Q}_1 \in \mathbb{M}_1^h$ with $\tau_h = \mathbf{div}_h \mathbf{Q}_1 \in \Gamma_h$,

$$\int_K \mathbf{Q}_1 : \epsilon(\zeta_2) \, d\mathbf{x} + \int_K \tau_h \cdot \zeta_2 \, d\mathbf{x} = 0 \quad \text{for all } \zeta_2 \text{ given in (4.31)}. \quad (4.33)$$

This condition indicates that, for all $\mathbf{Q}_h = \mathbf{Q}_0 + \mathbf{Q}_1 \in \mathbb{M}_0^h \oplus \mathbb{M}_1^h$ with $\tau_h = \mathbf{div}_h \mathbf{Q}_1 \in \Gamma_h$, it holds

$$b(\mathbf{Q}_h, \tau_h; v_h, \zeta_h)|_K = \int_K \mathbf{Q}_h : \epsilon(\zeta_h) \, d\mathbf{x} - \int_K \tau_h \cdot (\nabla v_h - \zeta_h) \, d\mathbf{x} \\ = \int_K \mathbf{Q}_0 : \epsilon(\zeta_2) \, d\mathbf{x} - \int_K \tau_h \cdot (\nabla v_h - \zeta_1) \, d\mathbf{x} \\ \text{for all } (v_h, \zeta_h) \in W_h \times \Theta_h. \quad (4.34)$$

Remark 4.8. Notice that \mathbf{Q}_0 and τ_h are uncoupled in (4.34), while \mathbf{Q}_h and τ_h are coupled. This uncoupled formulation is helpful to the verification of the inf-sup inequality (3.12) (see Section 4.3).

We are now at a position to construct \mathbb{M}_1^h . We first set

$$\mathbf{Q}_1|_K = \mathbf{Q}_1^{(1)} + \mathbf{Q}_1^{(2)} = (\widehat{\mathbf{Q}}_1^{(1)} + \widehat{\mathbf{Q}}_1^{(2)}) \circ F_K^{-1} \quad (4.35)$$

with

$$\widehat{\mathbf{Q}}_1^{(1)} \in (\text{span}\{\bar{\xi}, \bar{\xi}^2\}, \text{span}\{\bar{\eta}, \bar{\eta}^2\}, \text{span}\{\bar{\xi}^2, \bar{\eta}^2\})^T, \\ \widehat{\mathbf{Q}}_1^{(2)} = \Phi_0(\bar{c}_1, \dots, \bar{c}_5)^T. \quad (4.36)$$

Here the matrix Φ_0 is the same as in (4.25), and the parameters \bar{c}_i are to be determined. Notice that $\mathbf{Q}_1^{(2)} \in \mathbb{M}_0^h$ and it holds $\mathbf{div}_h \mathbf{Q}_1^{(2)} = 0$. Then, by the assumption (H1) and the relations (4.26) and (4.27), we set

$$\mathbf{div}_h \mathbf{Q}_1^{(1)} = \tau_h \text{ for } \tau_h \in \Gamma_h. \quad (4.37)$$

In view of the stress form (4.21), some calculations yield

$$\widehat{\mathbf{Q}}_1^{(1)} = J_0 \begin{pmatrix} \frac{1}{b_2} \bar{\zeta} - \frac{b_{12}}{2b_2^2} \bar{\zeta}^2 & \frac{a_{12}}{2b_2^2} \bar{\zeta}^2 & 0 & \frac{a_2}{b_2} \bar{\zeta}^2 \\ \frac{b_{12}}{2a_1^2} \bar{\eta}^2 & \frac{1}{a_1} \bar{\eta} - \frac{a_{12}}{2a_1^2} \bar{\eta}^2 & 0 & \frac{b_1}{a_1} \bar{\eta}^2 \\ 0 & 0 & \frac{1}{2a_1} \bar{\eta}^2 & \frac{1}{2b_2} \bar{\zeta}^2 \end{pmatrix} \begin{pmatrix} \bar{c}_1 \\ \vdots \\ \bar{c}_4 \end{pmatrix} =: \Phi_1 \begin{pmatrix} \bar{c}_1 \\ \vdots \\ \bar{c}_4 \end{pmatrix}, \tag{4.38}$$

where $(\bar{c}_1, \dots, \bar{c}_4)$ are the same parameters as in (4.21) for $\tau_h \in \Gamma_h$.

Remark 4.9. In fact, to fulfill the equilibrium relation (4.37) one may choose a different kind of basis function from that in (4.36) for $\widehat{\mathbf{Q}}_1^{(1)}$.

From (4.33) and (4.37), we have

$$\int_K \mathbf{Q}_1^{(2)} : \epsilon(\zeta_2) d\mathbf{x} = - \int_K \mathbf{Q}_1^{(1)} : \epsilon(\zeta_2) d\mathbf{x} - \int_K \tau_h \cdot \zeta_2 d\mathbf{x} \tag{4.39}$$

$$\Phi_2 = \begin{pmatrix} \left(\frac{J_0}{b_2} - \frac{a_2^2 b_1^2}{J_0 b_2} \right) \zeta + \frac{a_2^2 b_1}{J_0} \eta & \frac{a_2^3}{J_0} \zeta - \frac{a_1 a_2^2}{J_0} \eta & -\frac{a_2}{3} & - \left(\frac{a_2 J_0}{3b_2^2} + \frac{a_1 a_2}{3b_2} \right) + \frac{a_2 J_0}{b_2^2} \zeta^2 \\ -\frac{b_1^2 b_2}{J_0} \zeta + \frac{b_1^3}{J_0} \eta & \frac{a_2 b_2^2}{J_0} \zeta + \left(\frac{J_0}{a_1} - \frac{a_2^2 b_1^2}{J_0 a_1} \right) \eta & -\frac{b_1 b_2}{3a_1} - \frac{b_1 J_0}{3a_1^2} & - \left(\frac{b_1 J_0}{3a_1^2} + \frac{a_2 b_1^2}{3a_1 b_2} \right) + \frac{b_1 J_0}{a_1^2} \eta^2 \\ -\frac{a_2 b_1^2}{J_0} \zeta + \frac{a_1 b_1^2}{J_0} \eta & \frac{a_2^2 b_2}{J_0} \zeta - \frac{a_2^2 b_1}{J_0} \eta & -\frac{J_0}{6a_1} - \frac{b_2}{3} + \frac{J_0}{2a_1} \eta^2 & - \left(\frac{J_0}{6b_2} + \frac{a_2 b_1}{3b_2} \right) + \frac{J_0}{2b_2} \zeta^2 \end{pmatrix}. \tag{4.44}$$

for all ζ_2 given in (4.31). This, together with (4.31), (4.32), (4.38) and (4.21), leads to a linear system like

$$H_1(\bar{c}_1, \dots, \bar{c}_5)^T = -H_2(\bar{c}_1, \dots, \bar{c}_4)^T \tag{4.40}$$

with

$$H_1 = \int_K \mathbf{B}^T \Phi_0 d\mathbf{x} = \int_{-1}^1 \int_{-1}^1 J_K \mathbf{B}^T \Phi_0 d\xi d\eta,$$

$$H_2 = \int_K (\mathbf{B}^T \Phi_1 + \Phi_r^T \Phi_s) d\mathbf{x} = \int_{-1}^1 \int_{-1}^1 J_K (\mathbf{B}^T \Phi_1 + \Phi_r^T \Phi_s) d\xi d\eta.$$

Remark 4.10. Some simple calculations show

$$H_1 = \begin{pmatrix} 4b_2 & 0 & -4a_2 & 0 & -\frac{4}{3} \frac{a_2 J_2}{b_2^2} \\ -4b_1 & 0 & 4a_1 & -\frac{4}{3} \frac{J_1}{a_1} & 0 \\ 0 & 0 & 0 & \frac{4}{3} \frac{J_0}{a_1} & \frac{4}{3} \frac{a_2 J_0}{b_2^2} \\ 0 & 4a_1 & -4b_1 & -\frac{4}{3} \frac{a_1 J_1}{a_1^2} & 0 \\ 0 & 0 & 0 & \frac{4}{3} \frac{b_1 J_0}{a_1^2} & \frac{4}{3} \frac{J_0}{b_2} \end{pmatrix},$$

$$H_2 = \begin{pmatrix} \frac{4}{3} J_1 - \frac{2}{3} \frac{b_{12}}{b_2} \frac{J_0^2 + J_2^2}{J_0} & \frac{2}{3} \frac{a_{12}}{b_2} \frac{3J_0^2 + J_2^2}{3J_0} & -\frac{2}{3} \frac{a_2}{a_1} \frac{J_0^2 + J_1^2}{J_0} & \frac{2a_2}{b_2} \frac{3J_0^2 + J_2^2}{3J_0} \\ \frac{4}{3} J_2 + \frac{2}{3} \frac{b_1 b_{12}}{b_2^2} \frac{3J_0^2 + J_2^2}{3J_0} & -\frac{2}{3} \frac{a_{12} b_1}{b_2^2} \frac{J_0^2 + J_2^2}{J_0} & \frac{2(3J_0^2 + J_1^2)}{3J_0} & \frac{2}{3} \frac{J_0 - a_2 b_1}{b_2^2} \frac{J_0^2 + J_2^2}{J_0} \\ -\frac{4}{3} \frac{b_1 J_0 + b_{12} J_2}{b_2} & \frac{4}{3} \frac{a_{12} J_2}{b_2} & \frac{4}{3} J_1 & \frac{4}{3} \frac{a_2 J_2}{b_2} \\ \frac{2b_{12}}{a_1} \frac{3J_0^2 + J_2^2}{3J_0} & \frac{4}{3} J_2 - \frac{2}{3} \frac{a_{12}}{a_1} \frac{J_0^2 + J_2^2}{J_0} & \frac{2}{3} \frac{b_1}{a_1} \frac{3J_0^2 + J_1^2}{3J_0} & \frac{4}{3} \frac{b_1}{a_1} \frac{3J_0^2 + J_1^2}{3J_0} - \frac{2}{3} \frac{b_1}{b_2} \frac{J_0^2 + J_2^2}{J_0} \\ \frac{4}{3} \frac{b_{12} J_1}{a_1} & -\frac{4}{3} \frac{a_2 J_0 + a_{12} J_1}{a_1} & \frac{4}{9} \frac{b_1 J_1}{a_1} & \frac{4}{3} \frac{2b_1 J_1 + 3a_1 J_2}{3a_1} \end{pmatrix}.$$

In applications, it is not necessary to use these explicit forms of H_1 and H_2 .

In view of (4.13), it follows $\det(H_1) = \frac{4^5}{3^2} \frac{J_0^4}{a_1 b_2^2} > 0$, and (4.40) implies

$$(\bar{c}_1, \dots, \bar{c}_5)^T = -H_1^{-1} H_2(\bar{c}_1, \dots, \bar{c}_4)^T. \tag{4.41}$$

To sum up (4.23)–(4.25)(4.35), (4.38) and (4.41), a coupled moment/stress field $(\mathbf{Q}_h, \tau_h = \mathbf{div}_h \mathbf{Q}_h) \in \mathbb{M}_h \times \Gamma_h$ has the following forms, for $K \in T_h$,

$$\widehat{\mathbf{Q}} = \mathbf{Q}_h|_K \circ F_K = \Phi_0(c_1, \dots, c_5)^T + \Phi_2(\bar{c}_1, \dots, \bar{c}_4)^T, \tag{4.42}$$

$$\hat{\tau} = \tau_h|_K \circ F_K = \mathbf{div} \Phi_1(\bar{c}_1, \dots, \bar{c}_4)^T = \Phi_s(\bar{c}_1, \dots, \bar{c}_4)^T, \tag{4.43}$$

where $\Phi_2 := \Phi_1 - \Phi_0 H_1^{-1} H_2$, $c_i, \bar{c}_j \in \mathbb{R} (i = 1, \dots, 5; j = 1, \dots, 4)$, and Φ_0, Φ_1, Φ_s are defined respectively in (4.25), (4.38), (4.21).

Remark 4.11. When K is a parallelogram, it holds $a_{12} = b_{12} = 0$ and $J_1 = J_2 = 0$. Then it is to show Φ_2 has the form

4.3. Verification of the assumptions and uniform results

From the construction of the spaces $\mathbb{M}_h \times \Gamma_h$ (cf. (4.20), (4.23–4.26), (4.35) or their equivalent forms (4.42) and (4.43)), we see that the assumptions **(H1)**, **(H2)**, **(H4')** are fulfilled. The first and third approximation results of **(H5)**, i.e., (3.20) and (3.22), are standard for the piecewise bilinear approximation spaces W_h in (4.15) and \mathcal{O}_h in (4.16) at shape-regular meshes.

To verify the remaining assumptions, we introduce an additional mesh condition.

Condition (B) [40]. *The distance $d_K = |O_1 O_2| (|O_1 O_2| = \sqrt{a_{12}^2 + b_{12}^2})$; cf. (4.8)) between the midpoints of the diagonals of $K \in T_h$ is of order $O(h_K^2)$ uniformly for all elements $K \in T_h$ as $h \rightarrow 0$.*

Since $\widehat{P} := \{ \hat{v} = v|_K \circ F_K : v \in W_h \oplus B_h \} \supseteq P_2(\xi, \eta)$ and $\widehat{P} \not\supseteq Q_2(\xi, \eta)$ for $K \in T_h$, the second approximation result of **(H5)**, namely the estimate (3.21), only holds for asymptotically parallelogram, shape regular meshes [6,37]. Here, a family of quadrilateral meshes is called asymptotically parallelogram if it satisfies the angle condition $\sigma_K = O(h_K)$, namely if σ_K/h_K is uniformly bounded for all the elements in all the meshes, where $\sigma_K := \max(|\pi - \theta_1|, |\pi - \theta_2|)$ denotes the deviation of a quadrilateral from a parallelogram with θ_1 the angle between the outward normals of two opposite sides of K and θ_2 the angle between the outward normals of the other two sides. In [22] the Angle Condition, under the shape regular condition (4.2) and assuming h is sufficiently small, was shown to be equivalent to Condition (B), or the Bi-section Condition. The Angle Condition or Condition (B) ensures that the mesh subdivisions will converge to a set of parallelograms, and they will automatically hold when mesh subdivisions are constructed by bisections. We also refer to [33] for equivalence of several well-known shape regular mesh conditions.

It remains to verify the assumption **(H3)**.

Theorem 4.1. *Under Condition (B), the assumption **(H3)** holds, namely for all $(v_h, \zeta_h) \in W_h \times \mathcal{O}_h$, the following discrete inf-sup condition (3.12) holds.*

Remark 4.12. Notice that Condition (B) states

$$\max\{|a_{12}|, |b_{12}|\} = O(h_K^2), \quad \max\{|J_1|, |J_2|\} = O(h_K^3). \quad (4.45)$$

Recall the element geometric properties (4.13) and (4.14), namely

$$a_1 \approx b_2 \approx h_K, \quad \max\{a_2, b_1\} = O(h_K), \quad J_0 \approx h_K^2. \quad (4.46)$$

This allows us to view all the terms involving one of the factors a_{12} , b_{12}, J_1, J_2 as higher-order terms. Thus, under Condition (B) it remains to prove Theorem 4.1 in the case of parallelogram meshes.

According to Remark 4.12, in the analysis below we assume $K \in T_h$ is a parallelogram, and it follows:

$$a_{12} = b_{12} = 0, \quad J_1 = J_2 = 0.$$

Then, for any $\zeta_h \in \Theta_h$, from (4.29)–(4.32) we have $\zeta_h|_K = \zeta_1 + \zeta_2 = (\hat{\zeta}_1 + \hat{\zeta}_2) \circ F_K^{-1}$ with

$$\hat{\zeta}_1 = \begin{pmatrix} \bar{\zeta}_7 - \frac{1}{J_0}(b_1\bar{\zeta} + b_2\eta)\bar{\zeta}_6 \\ \bar{\zeta}_8 + \frac{1}{J_0}(a_1\bar{\zeta} + a_2\eta)\bar{\zeta}_6 \end{pmatrix}, \quad \hat{\zeta}_2 = \begin{pmatrix} \bar{\zeta}_1\bar{\zeta} + \bar{\zeta}_2\eta + \bar{\zeta}_3\bar{\zeta}\eta \\ \bar{\zeta}_4\eta + \bar{\zeta}_5\bar{\zeta}\eta \end{pmatrix} \text{ for } \bar{\zeta}_i \in \mathbb{R} \quad (4.47)$$

and

$$\epsilon(\zeta_h)|_K = \epsilon(\zeta_2) = \frac{1}{J_0} \begin{pmatrix} b_2\bar{\zeta}_1 - b_1\bar{\zeta}_2 - (b_1\bar{\zeta} - b_2\eta)\bar{\zeta}_3 \\ a_1\bar{\zeta}_4 + (a_1\bar{\zeta} - a_2\eta)\bar{\zeta}_5 \\ -a_2\bar{\zeta}_1 + a_1\bar{\zeta}_2 + (a_1\bar{\zeta} - a_2\eta)\bar{\zeta}_3 - b_1\bar{\zeta}_4 - (b_1\bar{\zeta} - b_2\eta)\bar{\zeta}_5 \end{pmatrix}. \quad (4.48)$$

Lemma 4.2. For any parallelogram $K \in T_h$ and ζ_2 from (4.47), it holds

$$h_K \|\epsilon(\zeta_h)\|_{0,K} = h_K \|\epsilon(\zeta_2)\|_{0,K} \approx \|\zeta_2\|_{0,K} \approx \left(\sum_{1 \leq i \leq 5} \bar{\zeta}_i^2 \right)^{1/2}. \quad (4.49)$$

Proof. In light of (4.46), we deduce

$$\begin{aligned} \|\zeta_2\|_{0,K}^2 &= \int_K \zeta_2 \cdot \zeta_2 \, d\mathbf{x} \\ &= J_0 \int_K \left[(\bar{\zeta}_1\bar{\zeta} + \bar{\zeta}_2\eta + \bar{\zeta}_3\bar{\zeta}\eta)^2 + (\bar{\zeta}_4\eta + \bar{\zeta}_5\bar{\zeta}\eta)^2 \right] d\xi d\eta \\ &= \frac{4}{3} J_0 \left(\bar{\zeta}_1^2 + \bar{\zeta}_2^2 + \frac{1}{3}\bar{\zeta}_3^2 + \bar{\zeta}_4^2 + \frac{1}{3}\bar{\zeta}_5^2 \right) \\ &\approx h_K^2 (\bar{\zeta}_1^2 + \bar{\zeta}_2^2 + \bar{\zeta}_3^2 + \bar{\zeta}_4^2 + \bar{\zeta}_5^2), \end{aligned} \quad (4.50)$$

$$\begin{aligned} h_K^2 \|\epsilon(\zeta_2)\|_{0,K}^2 &\approx J_0 \|\epsilon(\zeta_2)\|_{0,K}^2 = J_0 \int_K \epsilon(\zeta_2) : \epsilon(\zeta_2) \, d\mathbf{x} \\ &= \int_K \left[(b_2\bar{\zeta}_1 - b_1\bar{\zeta}_2 - (b_1\bar{\zeta} - b_2\eta)\bar{\zeta}_3)^2 + (a_1\bar{\zeta}_4 + (a_1\bar{\zeta} - a_2\eta)\bar{\zeta}_5)^2 \right. \\ &\quad \left. + \frac{1}{2}(-a_2\bar{\zeta}_1 + a_1\bar{\zeta}_2 + (a_1\bar{\zeta} - a_2\eta)\bar{\zeta}_3 - b_1\bar{\zeta}_4 - (b_1\bar{\zeta} - b_2\eta)\bar{\zeta}_5)^2 \right] \\ &\quad \times d\xi d\eta = 4 \left[(b_2\bar{\zeta}_1 - b_1\bar{\zeta}_2)^2 + \frac{1}{2}(a_2\bar{\zeta}_1 - a_1\bar{\zeta}_2 + b_1\bar{\zeta}_4)^2 + a_1^2\bar{\zeta}_4^2 \right] \\ &\quad + 4 \left[\left(\frac{b_1^2 + b_2^2}{3} + \frac{a_1^2 + a_2^2}{6} \right) \bar{\zeta}_3^2 + \left(\frac{a_1^2 + a_2^2}{3} + \frac{b_1^2 + b_2^2}{6} \right) \bar{\zeta}_5^2 \right. \\ &\quad \left. - \frac{a_1 b_1 + a_2 b_2}{3} \bar{\zeta}_3 \bar{\zeta}_5 \right] =: 4(\alpha_1 + \alpha_2). \end{aligned} \quad (4.51)$$

A combination with (4.46) and Cauchy inequality leads to

$$h_K \|\epsilon(\zeta_2)\|_{0,K} \lesssim \|\zeta_2\|_{0,K}.$$

In what follows, it suffices to prove

$$\|\zeta_2\|_{0,K} \lesssim h_K \|\epsilon(\zeta_2)\|_{0,K}. \quad (4.52)$$

To this end, we set $z_1 := b_2\bar{\zeta}_1 - b_1\bar{\zeta}_2$, $z_2 := a_2\bar{\zeta}_1 - a_1\bar{\zeta}_2 + b_1\bar{\zeta}_4$ to obtain

$$\begin{pmatrix} \bar{\zeta}_1 \\ \bar{\zeta}_2 \end{pmatrix} = \frac{1}{J_0} \begin{pmatrix} a_1 & -b_1 \\ a_2 & -b_2 \end{pmatrix} \begin{pmatrix} z_1 \\ z_2 - b_1\bar{\zeta}_4 \end{pmatrix}.$$

These relations, together with (4.46), some Cauchy inequality, and the definition of α_1 in (4.51), yield

$$h_K^2 (\bar{\zeta}_1^2 + \bar{\zeta}_2^2) \lesssim z_1^2 + \frac{z_2^2}{2} + a_1^2 \bar{\zeta}_4^2 = \alpha_1. \quad (4.53)$$

On the other hand, the inequality $abXY \leq \frac{1}{4}(a^2 + b^2)(X^2 + Y^2)$ implies

$$(a_1 b_1 + a_2 b_2) \bar{\zeta}_3 \bar{\zeta}_5 \leq \frac{1}{4} (a_1^2 + b_1^2 + a_2^2 + b_2^2) (\bar{\zeta}_3^2 + \bar{\zeta}_5^2).$$

Then from (4.46) and the definition of α_2 in (4.51), it follows:

$$h_K^2 (\bar{\zeta}_3^2 + \bar{\zeta}_5^2) \approx \frac{1}{12} (a_1^2 + b_1^2 + a_2^2 + b_2^2) (\bar{\zeta}_3^2 + \bar{\zeta}_5^2) \leq \alpha_2. \quad (4.54)$$

A combination of (4.50), (4.51), (4.53) and (4.54) yields (4.52). \square

In view of (4.23)–(4.25) (4.35), (4.42), (4.43) and Remark 4.11, for $\mathbf{Q}_h \in \mathbb{M}_h = \mathbb{M}_0^h \oplus \mathbb{M}_1^h$ with $\boldsymbol{\tau}_h = \mathbf{div}_h \mathbf{Q}_h \in \Gamma_h$, we have

$$\mathbf{Q}_h|_K = \mathbf{Q}_0 + \mathbf{Q}_1 \in \mathbb{M}_0^h|_K \oplus \mathbb{M}_1^h|_K,$$

where

$$\begin{aligned} \hat{\mathbf{Q}}_0 &= \mathbf{Q}_0 \circ F_K = \begin{pmatrix} 1 & 0 & 0 & \eta & \frac{a_2}{b_2} \bar{\zeta} \\ 0 & 1 & 0 & \frac{b_1}{a_1} \eta & \bar{\zeta} \\ 0 & 0 & 1 & \frac{b_1}{a_1} \eta & \frac{a_2}{b_2} \bar{\zeta} \end{pmatrix} \begin{pmatrix} \bar{c}_1 \\ \vdots \\ \bar{c}_5 \end{pmatrix}, \\ \hat{\mathbf{Q}}_1 &= \mathbf{Q}_1 \circ F_K = \Phi_2 \begin{pmatrix} \bar{c}_1 \\ \vdots \\ \bar{c}_4 \end{pmatrix} \end{aligned} \quad (4.55)$$

with Φ_2 from (4.44) and

$$\hat{\boldsymbol{\tau}} = \boldsymbol{\tau}_h|_K \circ F_K = \mathbf{div} \Phi_2 \begin{pmatrix} \bar{c}_1 \\ \vdots \\ \bar{c}_4 \end{pmatrix} = \begin{pmatrix} 1 & 0 & \eta & \frac{a_2}{b_2} \bar{\zeta} \\ 0 & 1 & \frac{b_1}{a_1} \eta & \bar{\zeta} \end{pmatrix} \begin{pmatrix} \bar{c}_1 \\ \vdots \\ \bar{c}_4 \end{pmatrix}. \quad (4.56)$$

Lemma 4.3. For any parallelogram $K \in T_h$ and $(\boldsymbol{\tau}_h, \mathbf{Q}_1)$ with (4.55) and (4.56), it holds

$$h_K \|\boldsymbol{\tau}_h\|_{0,K} \approx \|\mathbf{Q}_1\|_{0,K} \approx h_K^2 \left(\sum_{1 \leq i \leq 4} \bar{c}_i^2 \right)^{1/2}. \quad (4.57)$$

Proof. Since $\boldsymbol{\tau}_h = \mathbf{div}_h \mathbf{Q}_h = \mathbf{div}_h \mathbf{Q}_1$, an inverse inequality implies

$$h_K \|\boldsymbol{\tau}_h\|_{0,K} \lesssim h_K \|\mathbf{Q}_1\|_{1,K} \lesssim \|\mathbf{Q}_1\|_{0,K}.$$

Then it suffices to prove

$$\|\mathbf{Q}_1\|_{0,K} \lesssim h_K \|\boldsymbol{\tau}_h\|_{0,K}. \quad (4.58)$$

Some simple calculations plus (4.46) yield

$$\begin{aligned} \|\boldsymbol{\tau}_h\|_{0,K}^2 &= \int_K \boldsymbol{\tau}_h \cdot \boldsymbol{\tau}_h \, d\mathbf{x} = J_0 \int_K \left((\bar{c}_1 + \bar{c}_3\eta + \bar{c}_4 \frac{a_2}{b_2} \bar{\zeta})^2 \right. \\ &\quad \left. + (\bar{c}_2 + \bar{c}_3 \frac{b_1}{a_1} \eta + \bar{c}_4 \bar{\zeta})^2 \right) d\xi d\eta \\ &= 4J_0 \left(\bar{c}_1^2 + \bar{c}_2^2 + \frac{1}{3} \left(1 + \frac{b_1^2}{a_1^2} \right) \bar{c}_3^2 + \frac{1}{3} \left(1 + \frac{a_2^2}{b_2^2} \right) \bar{c}_4^2 \right) \\ &\approx h_K^2 (\bar{c}_1^2 + \bar{c}_2^2 + \bar{c}_3^2 + \bar{c}_4^2) \end{aligned}$$

and

$$\|\mathbf{Q}_1\|_{0,K}^2 = \int_K \mathbf{Q}_1 \cdot \mathbf{Q}_1 \, d\mathbf{x} \lesssim h_K^4 (\bar{c}_1^2 + \bar{c}_2^2 + \bar{c}_3^2 + \bar{c}_4^2).$$

Hence (4.58) follows. \square

Lemma 4.4. For any $\zeta_h \in \mathcal{O}_h$ and any parallelogram $K \in T_h$, there exists $\mathbf{Q}_0 \in \mathbb{M}_{0,K}^h$ such that

$$\int_K \mathbf{Q}_0 : \epsilon(\zeta_h) \, d\mathbf{x} = \|\mathbf{Q}_0\|_{0,K}^2 \approx \|\epsilon(\zeta_h)\|_{0,K}^2. \tag{4.59}$$

Proof. From the decomposition (4.29) of $\zeta_h \in \mathcal{O}_h$, the relations (4.59) are equivalent to

$$\int_K \mathbf{Q}_0 : \epsilon(\zeta_2) \, d\mathbf{x} = \|\mathbf{Q}_0\|_{0,K}^2 \approx \|\epsilon(\zeta_2)\|_{0,K}^2 \tag{4.60}$$

with ζ_2 given by (4.47).

In view of (4.55) and (4.56), some calculations show

$$\|\mathbf{Q}_0\|_{0,K}^2 = \begin{pmatrix} c_1 \\ \vdots \\ c_5 \end{pmatrix}^T J_0 \begin{pmatrix} 4 & 0 & 0 & 0 & 0 \\ 0 & 4 & 0 & 0 & 0 \\ 0 & 0 & 8 & 0 & 0 \\ 0 & 0 & 0 & \frac{4}{3} \left(1 + 2\left(\frac{b_1}{a_1}\right)^2 + \left(\frac{b_1^2}{a_1^2}\right)^2\right) & 0 \\ 0 & 0 & 0 & 0 & \frac{4}{3} \left(1 + 2\left(\frac{a_2}{b_2}\right)^2 + \left(\frac{a_2^2}{b_2^2}\right)^2\right) \end{pmatrix} \begin{pmatrix} c_1 \\ \vdots \\ c_5 \end{pmatrix},$$

$$\int_K \mathbf{Q}_0 : \epsilon(\zeta_2) \, d\mathbf{x} = \begin{pmatrix} c_1 \\ \vdots \\ c_5 \end{pmatrix}^T \begin{pmatrix} 4b_2 & -4b_1 & 0 & 0 & 0 \\ 0 & 0 & 0 & 4a_1 & 0 \\ -4a_2 & 4a_1 & 0 & -4b_1 & 0 \\ 0 & 0 & \frac{4}{3} \frac{J_0}{a_1} & 0 & \frac{4}{3} \frac{b_1}{a_1} \frac{J_0}{a_1} \\ 0 & 0 & \frac{4}{3} \frac{a_2}{b_2} \frac{J_0}{b_2} & 0 & \frac{4}{3} \frac{J_0}{b_2} \end{pmatrix} \begin{pmatrix} \bar{\zeta}_1 \\ \vdots \\ \bar{\zeta}_5 \end{pmatrix}.$$

The substitution of

$$\begin{aligned} \begin{pmatrix} c_1 \\ \vdots \\ c_5 \end{pmatrix} &= \frac{1}{J_0} \text{diag} \left(\frac{1}{4}, \frac{1}{4}, \frac{1}{8}, \frac{3}{8}, \frac{a_1^4}{a_1^4 + 2a_1^2 b_1^2 + b_1^4}, \frac{3}{4}, \frac{b_2^4}{a_2^4 + 2a_2^2 b_2^2 + b_2^4} \right) \\ &\times \begin{pmatrix} 4b_2 & -4b_1 & 0 & 0 & 0 \\ 0 & 0 & 0 & 4a_1 & 0 \\ -4a_2 & 4a_1 & 0 & -4b_1 & 0 \\ 0 & 0 & \frac{4}{3} \frac{J_0}{a_1} & 0 & \frac{4}{3} \frac{b_1}{a_1} \frac{J_0}{a_1} \\ 0 & 0 & \frac{4}{3} \frac{a_2}{b_2} \frac{J_0}{b_2} & 0 & \frac{4}{3} \frac{J_0}{b_2} \end{pmatrix} \begin{pmatrix} \bar{\zeta}_1 \\ \vdots \\ \bar{\zeta}_5 \end{pmatrix} \\ &= \frac{1}{J_0} \begin{pmatrix} b_2 & -b_1 & 0 & 0 & 0 \\ 0 & 0 & 0 & a_1 & 0 \\ -\frac{a_2}{2} & \frac{a_1}{2} & 0 & -\frac{b_1}{2} & 0 \\ 0 & 0 & \frac{J_0 a_1^3}{a_1^4 + 2a_1^2 b_1^2 + b_1^4} & 0 & \frac{J_0 a_1^2 b_1}{a_1^4 + 2a_1^2 b_1^2 + b_1^4} \\ 0 & 0 & \frac{J_0 a_2 b_2^3}{a_2^4 + 2a_2^2 b_2^2 + b_2^4} & 0 & \frac{J_0 b_2^3}{a_2^4 + 2a_2^2 b_2^2 + b_2^4} \end{pmatrix} \begin{pmatrix} \bar{\zeta}_1 \\ \vdots \\ \bar{\zeta}_5 \end{pmatrix} \\ &= \frac{1}{J_0} \begin{pmatrix} b_2 \bar{\zeta}_1 - b_1 \bar{\zeta}_2 \\ a_1 \bar{\zeta}_4 \\ \frac{1}{2} (-a_2 \bar{\zeta}_1 + a_1 \bar{\zeta}_2 - b_1 \bar{\zeta}_4) \\ \frac{J_0 a_1^2}{a_1^4 + 2a_1^2 b_1^2 + b_1^4} (a_1 \bar{\zeta}_3 + b_1 \bar{\zeta}_5) \\ \frac{J_0 b_2^3}{a_2^4 + 2a_2^2 b_2^2 + b_2^4} (a_2 \bar{\zeta}_3 + b_2 \bar{\zeta}_5) \end{pmatrix} =: \begin{pmatrix} Z_1 \\ Z_4 \\ Z_2 \\ Z_3 \\ Z_5 \end{pmatrix} \end{aligned} \tag{4.61}$$

into (4.55) leads to

$$\widehat{\mathbf{Q}}_0 = \begin{pmatrix} 1 & 0 & 0 & \eta & \frac{a_2^2}{b_2^2} \zeta \\ 0 & 1 & 0 & \frac{b_1^2}{a_1^2} \eta & \zeta \\ 0 & 0 & 1 & \frac{b_1}{a_1} \eta & \frac{a_2}{b_2} \zeta \end{pmatrix} \begin{pmatrix} Z_1 \\ Z_4 \\ Z_2 \\ Z_3 \\ Z_5 \end{pmatrix}$$

and

$$\int_K \mathbf{Q}_0 : \epsilon(\zeta_2) \, d\mathbf{x} = \|\mathbf{Q}_0\|_{0,K}^2. \tag{4.62}$$

On one hand, the element geometry properties (4.46) and the relations (4.49) and (4.50) imply

$$\|\mathbf{Q}_0\|_{0,K}^2 \approx h_K^2 \sum_{1 \leq i \leq 5} z_i^2 \lesssim \sum_{1 \leq i \leq 5} \bar{\zeta}_i^2 \approx \|\epsilon(\zeta_2)\|_{0,K}^2. \tag{4.63}$$

Moreover, (4.61) implies

$$\begin{aligned} \bar{\zeta}_4 &= \frac{J_0}{a_1} z_4, \quad \bar{\zeta}_1 = a_1 z_1 + b_1 \left(2z_2 + \frac{b_1}{a_1} z_4 \right), \quad \bar{\zeta}_2 = a_2 z_1 + b_2 \left(2z_2 + \frac{b_1}{a_1} z_4 \right), \\ \bar{\zeta}_3 &= b_2 \frac{a_1^4 + 2a_1^2 b_1^2 + b_1^4}{J_0 a_1^2} z_3 - b_1 \frac{a_2^4 + 2a_2^2 b_2^2 + b_2^4}{J_0 b_2^2} z_5, \\ \bar{\zeta}_5 &= -a_2 \frac{a_1^4 + 2a_1^2 b_1^2 + b_1^4}{J_0 a_1^2} z_3 + a_1 \frac{a_2^4 + 2a_2^2 b_2^2 + b_2^4}{J_0 b_2^2} z_5. \end{aligned}$$

Then from (4.46) it follows

$$\sum_{1 \leq i \leq 5} \bar{\zeta}_i^2 \lesssim h_K^2 \sum_{1 \leq i \leq 5} z_i^2.$$

A combination of the above inequality and (4.62) and (4.63) yields the desired conclusion. \square

Lemma 4.5. For any $v_h \in W_h$, $\zeta_h \in \mathcal{O}_h$ with ζ_1 from (4.47), and for any parallelogram $K \in T_h$, there exists $\tau_h \in \Gamma_h$ such that

$$\begin{aligned} \int_K \tau_h \cdot (\nabla v_h - \zeta_1) \, d\mathbf{x} &= -(t^2 + h^2) \|\tau_h\|_{0,K}^2 \\ &\approx -\frac{1}{t^2 + h^2} \|\nabla v_h - \zeta_1\|_{0,K}^2. \end{aligned} \tag{4.64}$$

Proof. We follow the same line as in the proof of Lemma 4.4. For $v_h \in W_h$, we assume $v_h|_K = (v_0 + v_1 \zeta + v_2 \eta + v_3 \zeta \eta) \circ F_K^{-1}$. Then from (4.47) it follows:

$$\nabla v - \zeta_1 = \frac{1}{J_0} \left((v_1 b_2 - v_2 b_1 - J_0 \bar{\zeta}_7) - (v_3 - \bar{\zeta}_6) b_1 \zeta + (v_3 + \bar{\zeta}_6) b_2 \eta \right) + \frac{1}{J_0} \left((v_2 a_1 - v_1 a_2 - J_0 \bar{\zeta}_8) + (v_3 - \bar{\zeta}_6) a_1 \zeta - (v_3 + \bar{\zeta}_6) a_2 \eta \right).$$

Denote $\bar{v}_1 := v_1 - a_1 \bar{\zeta}_7 - b_1 \bar{\zeta}_8$, $\bar{v}_2 := v_2 - a_2 \bar{\zeta}_7 - b_2 \bar{\zeta}_8$, $\bar{v}_3 := v_3 - \bar{\zeta}_6$, $\bar{v}_4 := v_3 + \bar{\zeta}_6$, we then have

$$\nabla v - \zeta_1 = \frac{1}{J_0} \begin{pmatrix} b_2 & -b_1 & -b_1 \zeta & b_2 \eta \\ -a_2 & a_1 & a_1 \zeta & -a_2 \eta \end{pmatrix} \begin{pmatrix} \bar{v}_1 \\ \vdots \\ \bar{v}_4 \end{pmatrix}.$$

This, together with the element geometric properties (4.46), yields

$$\begin{aligned} \|\nabla v - \zeta_1\|_{0,K}^2 &= \int_K (\nabla v - \zeta_1) \cdot (\nabla v - \zeta_1) \, dx \\ &= \frac{4}{J_0} \left((b_2 \bar{v}_1 - b_1 \bar{v}_2)^2 + (-a_2 \bar{v}_1 + a_1 \bar{v}_2)^2 \right. \\ &\quad \left. + \frac{1}{3} (a_1^2 + b_1^2) \bar{v}_3^2 + \frac{1}{3} (a_2^2 + b_2^2) \bar{v}_4^2 \right) \approx \sum_{1 \leq i \leq 4} \bar{v}_i^2. \end{aligned} \quad (4.65)$$

On the other hand, for $\tau_h \in \Gamma_h$, from (4.56) we have

$$\begin{aligned} \|\tau_h\|_0^2 &= \int_K \tau_h \cdot \tau_h \, dx \\ &= \begin{pmatrix} \bar{c}_1 \\ \vdots \\ \bar{c}_4 \end{pmatrix}^T J_0 \int_K \begin{pmatrix} 1 & 0 \\ \eta & \frac{b_1}{a_1} \eta \\ \frac{a_2}{b_2} \zeta & \zeta \end{pmatrix} \begin{pmatrix} 1 & 0 & \eta & \frac{a_2}{b_2} \zeta \\ 0 & 1 & \frac{b_1}{a_1} \eta & \zeta \end{pmatrix} d\zeta d\eta \begin{pmatrix} \bar{c}_1 \\ \vdots \\ \bar{c}_4 \end{pmatrix} \\ &= \begin{pmatrix} \bar{c}_1 \\ \vdots \\ \bar{c}_4 \end{pmatrix}^T 4J_0 \begin{pmatrix} 1 & 0 & 0 & 0 \\ 0 & 1 & 0 & 0 \\ 0 & 0 & \frac{1}{3} \left(1 + \frac{b_1^2}{a_1^2}\right) & 0 \\ 0 & 0 & 0 & \frac{1}{3} \left(1 + \frac{a_2^2}{b_2^2}\right) \end{pmatrix} \begin{pmatrix} \bar{c}_1 \\ \vdots \\ \bar{c}_4 \end{pmatrix} \\ &\approx h_K^2 \sum_{1 \leq i \leq 4} \bar{c}_i^2, \\ &\int_K \tau_h \cdot (\nabla v - \zeta_1) \, dx \\ &= \begin{pmatrix} \bar{c}_1 \\ \vdots \\ \bar{c}_4 \end{pmatrix}^T \int_K \begin{pmatrix} 1 & 0 \\ \eta & \frac{b_1}{a_1} \eta \\ \frac{a_2}{b_2} \zeta & \zeta \end{pmatrix} \begin{pmatrix} b_2 & -b_1 & -b_1 \zeta & b_2 \eta \\ -a_2 & a_1 & a_1 \zeta & -a_2 \eta \end{pmatrix} d\zeta d\eta \begin{pmatrix} \bar{v}_1 \\ \vdots \\ \bar{v}_4 \end{pmatrix} \\ &= \begin{pmatrix} \bar{c}_1 \\ \vdots \\ \bar{c}_4 \end{pmatrix}^T 4 \begin{pmatrix} b_2 & -b_1 & 0 & 0 \\ -a_2 & a_1 & 0 & 0 \\ 0 & 0 & 0 & \frac{1}{3} \frac{J_0}{a_1} \\ 0 & 0 & \frac{1}{3} \frac{J_0}{b_2} & 0 \end{pmatrix} \begin{pmatrix} \bar{v}_1 \\ \vdots \\ \bar{v}_4 \end{pmatrix}. \end{aligned} \quad (4.66)$$

The substitution of

$$\begin{aligned} \begin{pmatrix} \bar{c}_1 \\ \bar{c}_2 \\ \bar{c}_3 \\ \bar{c}_4 \end{pmatrix} &= -\frac{1}{(t^2 + h^2)J_0} \begin{pmatrix} 1 & 0 & 0 & 0 \\ 0 & 1 & 0 & 0 \\ 0 & 0 & \frac{3a_1^2}{a_1^2 + b_1^2} & 0 \\ 0 & 0 & 0 & \frac{3b_2^2}{a_2^2 + b_2^2} \end{pmatrix} \begin{pmatrix} b_2 & -b_1 & 0 & 0 \\ -a_2 & a_1 & 0 & 0 \\ 0 & 0 & 0 & \frac{1}{3} \frac{J_0}{a_1} \\ 0 & 0 & \frac{1}{3} \frac{J_0}{b_2} & 0 \end{pmatrix} \begin{pmatrix} \bar{v}_1 \\ \bar{v}_2 \\ \bar{v}_3 \\ \bar{v}_4 \end{pmatrix} \\ &= \frac{1}{(t^2 + h^2)J_0} \begin{pmatrix} b_2 & -b_1 & 0 & 0 \\ -a_2 & a_1 & 0 & 0 \\ 0 & 0 & 0 & \frac{J_0 a_1}{a_1^2 + b_1^2} \\ 0 & 0 & \frac{J_0 b_2}{a_2^2 + b_2^2} & 0 \end{pmatrix} \begin{pmatrix} \bar{v}_1 \\ \bar{v}_2 \\ \bar{v}_3 \\ \bar{v}_4 \end{pmatrix} \end{aligned} \quad (4.67)$$

into (4.56) leads to

$$\int_K \tau_h \cdot (\nabla v - \zeta_1) \, dx = -(t^2 + h^2) \|\tau_h\|_0^2. \quad (4.68)$$

Notice that (4.67) also implies

$$\sum_{1 \leq i \leq 4} \bar{c}_i^2 \approx \frac{1}{(t^2 + h^2)^2} \frac{1}{h_K^2} \sum_{1 \leq i \leq 4} \bar{v}_i^2.$$

Finally, a combination of (4.65), (4.66), (4.68) and the above relation ends the proof. \square

In light of Lemma 4.2, 4.3, 4.4, 4.5, we deduce the following inf-sup result for parallelogram meshes.

Theorem 4.2. Let T_h be a shape-regular triangulation of Ω into parallelograms. Then the assumption (H3) holds, namely for any $(v_h, \zeta_h) \in W_h \times \Theta_h$, it holds the discrete inf-sup condition

$$\|(v_h, \zeta_h)\|_{h,2} \lesssim \sup_{(\mathbf{Q}_h, \tau_h) \in \mathbb{M}_h \times \Gamma_h} \frac{b(\mathbf{Q}_h, \tau_h; v_h, \zeta_h)}{\|(\mathbf{Q}_h, \tau_h)\|_{h,1}}.$$

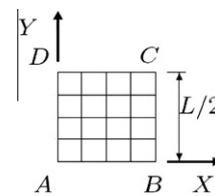
Proof. For $(v_h, \zeta_h) \in W_h \times \Theta_h$, let \mathbf{Q}_0 and $\tau_h = \text{div}_h \mathbf{Q}_1$ be the same as in Lemmas 4.4 and 4.5 with $\mathbf{Q}_h|_K = \mathbf{Q}_0 + \mathbf{Q}_1$. Notice that the relation (4.33) leads to the simplified form (4.34). Recalling the norm definitions (3.7) and (3.8), it suffices to show

$$\begin{aligned} &\left(\|\epsilon(\zeta_h)\|_0^2 + \frac{1}{t^2 + h^2} \|\nabla v_h - \zeta_h\|_0^2 \right)^{1/2} \\ &\lesssim \frac{\sum_{K \in T_h} \int_K (\mathbf{Q}_0 : \epsilon(\zeta_2) - \tau_h \cdot (\nabla v_h - \zeta_1)) \, dx}{\left(\|\mathbf{Q}_h\|_0^2 + (t^2 + h^2) \|\tau_h\|_0^2 \right)^{1/2}} =: R. \end{aligned} \quad (4.69)$$

Lemmas 4.4 and 4.5 show

$$\begin{aligned} R &\approx \frac{\sum_{K \in T_h} \left(\|\mathbf{Q}_0\|_{0,K}^2 + (t^2 + h^2) \|\tau_h\|_{0,K}^2 \right)}{\left[\|\mathbf{Q}_h\|_0^2 + (t^2 + h^2) \|\tau_h\|_0^2 \right]^{1/2}} \\ &\gtrsim \frac{\sum_{K \in T_h} \left(\|\mathbf{Q}_0\|_{0,K}^2 + (t^2 + h^2) \|\tau_h\|_{0,K}^2 \right)}{\left[\sum_{K \in T_h} \left(\|\mathbf{Q}_0\|_{0,K}^2 + \|\mathbf{Q}_1\|_{0,K}^2 + (t^2 + h^2) \|\tau_h\|_{0,K}^2 \right) \right]^{1/2}} \\ &\approx \frac{\sum_{K \in T_h} \left(\|\mathbf{Q}_0\|_{0,K}^2 + (t^2 + h^2) \|\tau_h\|_{0,K}^2 \right)}{\left[\sum_{K \in T_h} \left(\|\mathbf{Q}_0\|_{0,K}^2 + (t^2 + h^2) \|\tau_h\|_{0,K}^2 \right) \right]^{1/2}} \\ &= \left[\sum_{K \in T_h} \left(\|\mathbf{Q}_0\|_{0,K}^2 + (t^2 + h^2) \|\tau_h\|_{0,K}^2 \right) \right]^{1/2} \\ &\gtrsim \left[\sum_{K \in T_h} \left(\|\epsilon(\zeta_h)\|_{0,K}^2 + \frac{1}{h^2} \|\zeta_2\|_{0,K}^2 + \frac{1}{t^2 + h^2} \|\nabla v_h - \zeta_1\|_{0,K}^2 \right) \right]^{1/2} \\ &\gtrsim \left(\|\epsilon(\zeta_h)\|_0^2 + \frac{1}{t^2 + h^2} \|\nabla v_h - \zeta_h\|_0^2 \right)^{1/2}. \end{aligned}$$

This concludes the proof. \square



$E = 10920$; $\nu = 0.3$; $L = 10$
 uniform loading; $q = 1$
 Boundary conditions on BC & CD :
 For clamped plate: $\omega = \beta_s = \beta_n = 0$
 For SS2 plate: $\omega = \beta_s = 0$
 Symmetry conditions:
 $\beta_x = 0$ on AD and $\beta_y = 0$ on AB

Fig. 2. Quadrant of a square plate: geometry and 4×4 meshes.

Table 1

Results of central deflection $w_c(10^{-5}qL^4/D)$ and central moment $M_c(10^{-4}qL^2)$ computed by the new method for a clamped square plate with a uniform load discretized into 6×6 in different thickness/span ratios.

t	10^{-1}	10^{-4}	10^{-6}	10^{-9}	10^{-14}	Exact
w_c	130.6	130.4	130.4	130.4	130.4	126.5
M_c	240.5	240.5	240.5	240.5	240.5	231.0
M_c^*	231.1	231.1	231.1	231.1	231.1	

* Computed by $\mathcal{D}\epsilon(\beta_h)$.

Table 2
Central deflection $w_c(10^{-5}qL^4/D)$ and central moment $M_c(10^{-4}qL^2)$ for a simply-supported square plate with a uniform load discretized into 6×6 in different thickness/span ratios.

	t	2.5	2	0.5	10^{-1}	10^{-4}	10^{-6}	10^{-9}	10^{-14}
w_c	DKQ	406.1	406.1	406.1	406.1	406.1	406.1	406.1	406.1
	MITC4	537.6	490.0	410.6	405.5	405.3	417.0	0.000	0.000
	New	541.0	493.4	414.0	408.9	408.7	408.7	408.7	408.7
	Exact [10]	517.9	490.8	410.8	406.4	406.2	406.2	406.2	406.2
M_c	DKQ	481.0	481.0	481.0	481.0	481.0	481.0	481.0	481.0
	MITC4	478.9	478.9	478.9	478.9	478.9	495.5	417.1	0.090
	New	487.6	487.6	487.6	487.5	487.5	487.5	487.5	487.5
	New*	478.7	478.7	478.7	478.7	478.7	478.7	478.7	478.7
	Exact [10]	479.0	479.0	479.0	479.0	479.0	479.0	479.0	479.0

Table 3
Central deflection $w_c(10^{-5}qL^4/D)$, central moment $M_c(10^{-4}qL^2)$ for a clamped square plate (uniform load, $t = 0.1$) and a posteriori ratio r for the new method.

	w_c			M_c				r
	DKQ	MITC4	New	DKQ	MITC4	New	New*	
2×2	146.1	121.3	157.4	287.3	251.7	306.5	236.4	
4×4	131.9	125.3	135.2	243.3	233.1	253.9	233.3	0.66
8×8	127.9	126.4	129.0	232.6	230.1	235.6	230.3	0.78
16×16	-	-	127.3	231.3	229.7	230.7	229.4	0.87
32×32	-	-	126.9	231.3	229.7	229.5	229.2	0.94
Exact		126.5				231.0		

Theorem 4.1 follows from Theorem 4.2 and Remark 4.12.

In light of Lemma 3.2 and Theorem 3.2 we have the following convergence result.

Theorem 4.3. Under Condition (B) and the condition (3.26), the discretization problem (3.1) and (3.2) admits a unique solution $(\mathbf{M}_h, \gamma_h, w_h, \beta_h) \in \mathbb{M}_h \times \Gamma_h \times W_h \times \Theta_h$ such that the estimate (4.3) holds, namely

$$\|\mathbf{M} - \mathbf{M}_h\|_0 + (h+t)\|\gamma - \gamma_h\|_0 + \|\beta - \beta_h\|_1 + \|w - w_h\|_1 \lesssim h(\|\mathbf{M}\|_1 + t\|\gamma\|_1 + \|\gamma\|_0 + \|\beta\|_2 + \|w\|_3).$$

Table 4
Central deflection w_c , central moment M_c and a posteriori ratio r for the new method for a clamped square plate (uniform load).

		2×2	4×4	8×8	16×16	32×32	Exact
$t = 0.01$	w_c	157.1	135.0	128.7	127.1	126.7	126.5
	M_c	306.5	253.9	235.6	230.7	229.5	231.0
	M_c^*	236.5	233.3	230.3	229.4	229.1	231.0
	r		0.69	0.79	0.88	0.93	
$t = 0.0001$	w_c	157.1	135.0	128.7	127.1	126.7	126.5
	M_c	306.5	253.9	235.6	230.7	229.5	231.0
	M_c^*	236.5	233.3	230.3	229.4	229.1	231.0
	r		1.12	1.04	1.01	1.00	

Table 5
Central deflection w_c , central moment M_c and a posteriori ratio r for the new method for a simply-supported square plate (uniform load).

		2×2	4×4	8×8	16×16	32×32	Exact
$t = .01$	w_c	428.2	412.0	407.8	406.8	406.5	406.5
	M_c	546.6	498.1	483.8	480.1	479.2	479.0
	M_c^*	474.0	478.5	478.8	478.8	478.9	479.0
	r		0.55	0.84	0.93	0.97	
$t = 0.0001$	w_c	428.0	411.8	407.6	406.6	406.3	406.5
	M_c	546.6	498.1	483.8	480.1	479.2	479.0
	M_c^*	474.0	478.5	478.8	478.8	478.9	479.0
	r		0.59	0.85	0.94	0.97	
$t = 0.0001$	w_c	428.0	411.8	407.6	406.6	406.3	406.5
	M_c	546.6	498.1	483.8	480.1	479.2	479.0
	M_c^*	474.0	478.5	478.8	478.8	478.9	479.0
	r		0.99	1.00	1.00	1.00	

5. A posteriori error estimates

We follow the version of [21] to derive residual-based a posteriori error estimates. Define the residuals, for all $(\mathbf{Q}, \tau) \in \mathbb{M} \times \Gamma$ and $(v, \zeta) \in W \times \Theta$,

$$r_{\mathbb{M} \times \Gamma}(\mathbf{Q}, \tau) := a(\mathbf{M}_h, \gamma_h; \mathbf{Q}, \tau) + b(\mathbf{Q}, \tau; w_h, \beta_h),$$

$$r_{W \times \Theta}(v, \zeta) := - \int_{\Omega} g v d\mathbf{x} - b(\mathbf{M}_h, \gamma_h; v, \zeta),$$

where the bilinear forms $a(\cdot, \cdot; \cdot, \cdot)$ and $b(\cdot, \cdot; \cdot, \cdot)$ are given in (1.8) and (1.9). Theorem 2.1 leads to the following lemma.

Lemma 5.1. For the solution $(\mathbf{M}, \gamma, w, \beta) \in \mathbb{M} \times \Gamma \times W \times \Theta$ of the problem (2.1) and (2.2) and the discrete solution $(\mathbf{M}_h, \gamma_h, w_h, \beta_h) \in \mathbb{M}_h \times \Gamma_h \times W_h \times \Theta_h$ of the problem (3.1) and (3.2), it holds

$$\|(\mathbf{M} - \mathbf{M}_h, \gamma - \gamma_h)\|_{\mathbb{M} \times \Gamma} + \|(w - w_h, \beta - \beta_h)\|_{W \times \Theta} \approx \sup_{(\mathbf{Q}, \tau) \in \mathbb{M} \times \Gamma} \frac{r_{\mathbb{M} \times \Gamma}(\mathbf{Q}, \tau)}{\|(\mathbf{Q}, \tau)\|_{\mathbb{M} \times \Gamma}} + \sup_{(v, \zeta) \in W \times \Theta} \frac{r_{W \times \Theta}(v, \zeta)}{\|(v, \zeta)\|_{W \times \Theta}}. \tag{5.1}$$

The following two computable error estimators

$$\eta_{\mathbb{M} \times \Gamma}^2 := \sum_{K \in \mathcal{T}_h} \|\mathcal{D}^{-1} \mathbf{M}_h + \epsilon(\beta_h)\|_{0,K}^2 + t^2 \|\frac{1}{\lambda} \gamma_h - t^{-2}(\nabla w_h - \beta_h)\|_{0,K}^2, \tag{5.2}$$

$$\eta_{W \times \Theta}^2 := \sum_{K \in \mathcal{T}_h} h_K^2 \left(\|\operatorname{div} \boldsymbol{\gamma}_h + \mathbf{g}\|_{0,K}^2 + \|\operatorname{div} \mathbf{M}_h - \boldsymbol{\gamma}_h\|_{0,K}^2 \right) + \sum_{E \in \mathcal{E}_h^0} h_E \left(\|\boldsymbol{\gamma}_h \cdot \mathbf{n}\|_{0,E}^2 + \|\mathbf{M}_h \mathbf{n}\|_{0,E}^2 \right) \quad (5.3)$$

lead to a reliable a posteriori error estimate.

Theorem 5.1. Let $(\mathbf{M}, \boldsymbol{\gamma}, w, \boldsymbol{\beta}) \in \mathbb{M} \times \Gamma \times W \times \Theta$ and $(\mathbf{M}_h, \boldsymbol{\gamma}_h, w_h, \boldsymbol{\beta}_h) \in \mathbb{M}_h \times \Gamma_h \times W_h \times \Theta_h$ solve the problems (2.1), (2.2) and (3.1). Then it holds

$$\|(\mathbf{M} - \mathbf{M}_h, \boldsymbol{\gamma} - \boldsymbol{\gamma}_h)\|_{\mathbb{M} \times \Gamma} + \|(w - w_h, \boldsymbol{\beta} - \boldsymbol{\beta}_h)\|_{W \times \Theta} \lesssim \eta_{\mathbb{M} \times \Gamma} + \eta_{W \times \Theta}. \quad (5.4)$$

Proof. By Lemma 5.1 we only need to estimate the terms $r_{\mathbb{M} \times \Gamma}(\mathbf{Q}, \boldsymbol{\tau})$ and $r_{W \times \Theta}(v, \zeta)$. The Cauchy inequality implies

$$r_{\mathbb{M} \times \Gamma}(\mathbf{Q}, \boldsymbol{\tau}) \lesssim \eta_{\mathbb{M} \times \Gamma} \|(\mathbf{Q}, \boldsymbol{\tau})\|_{\mathbb{M} \times \Gamma}. \quad (5.5)$$

Let $(v_h, \zeta_h) \in W_h \times \Theta_h$ be the Clement-type interpolation of $(v, \zeta) \in W \times \Theta$ with

$$\sum_{K \in \mathcal{T}_h} h_K^{-2} \left(\|v - v_h\|_{0,K}^2 + \|\zeta - \zeta_h\|_{0,K}^2 \right) + \sum_{E \in \mathcal{E}_h} h_E^{-1} \left(\|v - v_h\|_{0,E}^2 + \|\zeta - \zeta_h\|_{0,E}^2 \right) \lesssim \|v\|_{1,\Omega}^2 + \|\zeta\|_{1,\Omega}^2 \approx \|(v, \zeta)\|_{W \times \Theta}^2. \quad (5.6)$$

The Galerkin orthogonality and an integration by parts imply

$$\begin{aligned} r_{W \times \Theta}(v, \zeta) &= - \int_{\Omega} \mathbf{g}(v - v_h) \, dx - \int_{\Omega} \mathbf{M}_h : \boldsymbol{\epsilon}(\zeta - \zeta_h) \, dx \\ &\quad + \int_{\Omega} \boldsymbol{\gamma}_h \cdot (\nabla(v - v_h) - (\zeta - \zeta_h)) \, dx \\ &= \sum_{K \in \mathcal{T}_h} \left(\int_K -(\operatorname{div} \boldsymbol{\gamma}_h + \mathbf{g})(v - v_h) \, dx \right. \\ &\quad \left. + \int_K (\operatorname{div} \mathbf{M}_h - \boldsymbol{\gamma}_h) \cdot (\zeta - \zeta_h) \, dx \right. \\ &\quad \left. + \sum_{E \in \mathcal{E}_h^0} \left(\int_E [\boldsymbol{\gamma}_h] \cdot \mathbf{n}(v - v_h) \, ds - \int_E [\mathbf{M}_h] \mathbf{n} \cdot (\zeta - \zeta_h) \, ds \right) \right). \end{aligned}$$

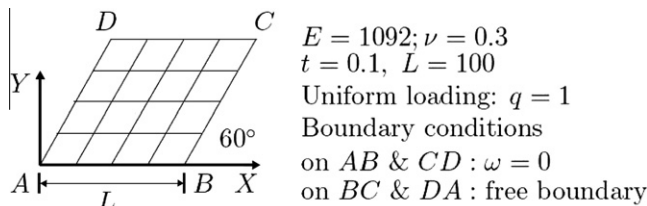


Fig. 3. Razaque's skew plate: geometry and 4 × 4 mesh.

Table 6 Results of central deflection $w_c(10^{-5}qL^4/D)$ and central moment $M_y(\times 10^{-3})$ for Razaque's skew plate (60°): $L/t = 1000$.

	w_c				M_y				r
	DKQ	MITC4	MiSP4	New	MITC4	MiSP4	New	New*	
2 × 2	0.6667	0.3856	0.5120	0.5655	0.3811	0.6066	0.9131	0.3636	
4 × 4	0.7696	0.6723	0.7259	0.7399	0.7722	0.8774	0.9290	0.7807	0.35
8 × 8	0.7877	0.7592	0.7781	0.7826	0.9076	0.9423	0.9567	0.9210	0.87
16 × 16	-	0.7827	0.7894	0.7912	0.9473	0.9567	0.9609	0.9524	0.97
32 × 32	-	0.7888	-	0.7928	0.9569	-	0.9613	0.9592	0.99
Exact		0.7945				0.9589			

The Cauchy–Schwarz inequality and (5.6) lead to

$$r_{W \times \Theta}(v, \zeta) \lesssim \eta_{W \times \Theta} \|(v, \zeta)\|_{W \times \Theta}. \quad (5.7)$$

A combination of (5.1), (5.5), and (5.7) yields the reliable a posteriori error estimate (5.4). □

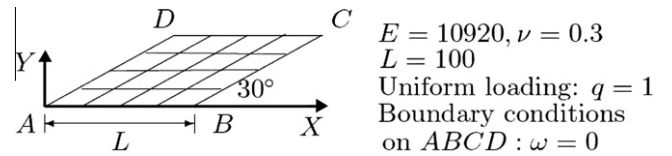


Fig. 4. Morley's acute skew plate: geometry and 4 × 4 mesh.

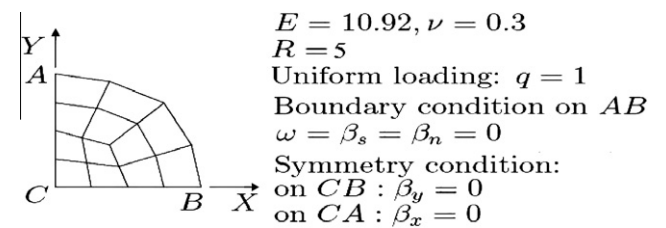


Fig. 5. 12-Element mesh of symmetric quadrant of a circular plate.

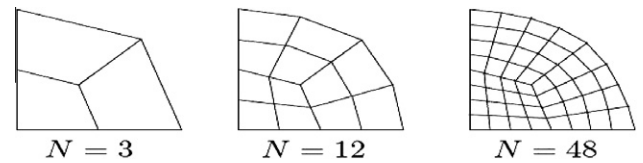


Fig. 6. Three meshes for quadrant of a circular plate.

Table 7 Central deflection $w_c(10^{-5}qL^4/D)$ for Moley's skew plate (30°) (Kirchhoff solution [34]: $w^f = 0.408$; 3D solution [8] at $t = 1$: $w^f = 0.424$).

		4 × 4	8 × 8	16 × 16	32 × 32
$t = 1$	w_c	DKQ 0.760	0.507	0.443	0.426
	r	MITC4 0.359	0.357	0.383	0.403
		New 0.446	0.434	0.427	0.424
$t = 0.1$	w_c	DKQ 0.760	0.507	0.443	0.423
	r	MITC4 0.358	0.343	0.343	0.359
		New 0.445	0.432	0.424	0.419
$t = 0.001$	w_c		0.82	0.96	0.97
	r	New 0.445	0.432	0.424	0.419
			0.83	0.96	0.98

Table 8
Central deflection w_c and central moment M_c for a clamped circular plate under uniform loading.

		$t = 1$			$t = 0.1$			$t = 0.001$		
		3	12	48	3	12	48	3	12	48
$w_c(t^3)$	DKQ	10.756	10.064	9.854	10.756	10.064	9.854	–	–	–
	MITC4	10.755	11.431	11.525	9.068	9.699	9.765	9.051	9.681	9.747
	New	12.635	12.079	11.701	10.899	10.286	9.930	10.881	10.267	9.912
	Exact		11.551			9.784			9.766	
M_c	DKQ	2.543	2.149	2.063	2.543	2.149	2.063	–	–	–
	MITC4	1.927	2.038	2.033	1.883	2.049	2.032	1.883	2.050	2.032
	New	2.325	2.156	2.069	2.348	2.124	2.063	2.348	2.122	2.062
	New*	1.578	1.968	2.015	1.578	1.981	2.018	1.577	1.981	2.018
	Exact		2.031			2.031		2.031		
r	New		0.93	0.97		0.98	0.99		1.03	1.05

6. Numerical results

The practical performance of the new scheme is investigated for a few benchmark tests in comparison with existing 4-node quadrilateral plate elements, namely the discrete Kirchhoff quadrilateral plate DKQ element [10], the MITC4 element [9], and the MiSP4 element [7].

6.1. Tests for locking

A clamped square plate and a simply supported plate with various range of thickness/span ratios subject to a uniform load (Fig. 2) are used to test the shear locking phenomenon. The results of central deflection and central moment presented in Tables 1 and 2 show that our method can avoid the shear locking phenomenon. Notice that for the experiments here and below, we use * to denote the corresponding bending moment result computed by $\mathcal{D}\epsilon(\beta_h)$.

6.2. A clamped/ simply supported square plate under a uniform load

Fig. 2 also shows a clamped/ simply supported square plate with various range of thickness/span ratios subjected to a uniform load. The results of central deflection, central moment and the a posteriori ratio

$$r = \log_2 \frac{(\eta_{M \times \Gamma} + \eta_{W \times \Theta})|_{h/2}}{(\eta_{M \times \Gamma} + \eta_{W \times \Theta})|_h}$$

between the mesh T_h and its bisection-refined mesh $T_{h/2}$ are reported in Tables 3–5. The new method gives convergent results for any given plate thickness t , and yields uniform results with the a posteriori ratio r close to 1 as t becomes small. Notice that we have shown in Theorem 5.1 that the a posteriori estimator $\eta_{M \times \Gamma} + \eta_{W \times \Theta}$ is reliable. So if it is also efficient, we can use r to denote the accuracy order of the new method. Theoretically, as shown in Theorem 4.3, the latter one is first order.

6.3. Razzaque's skew plate (60°) with two free edges

Fig. 3 shows the mesh generated for Razzaque skew plate (60°) subject to a uniform loading q [38]. The plate is simply supported on two opposite sides and free on the other two. The results in Table 6 shows that the new method is of good accuracy.

6.4. Morley's simply supported rhombic plate (30°) under a uniform loading

This test (Fig. 4) is a very critical one. Classically, Morley's solution is obtained using Kirchhoff theory [34]. Two aspect ratios

($L/t = 1000$ and 100) are considered. The case $L/t = 100$ was investigated by Babuska and Scapolla [8], in which it was considered as a full 3D-elastic problem. The results in Table 7 show that the new method is of uniformly good accuracy.

6.5. A clamped circular plate

Fig. 5 shows a clamped isotropic circular plate subjected to a uniform loading, which is used to demonstrate the versatility of the two proposed elements. A quarter of a plate with symmetry conditions on x - and y -axis is considered. Fig. 6 shows the used three kinds of finite element meshes.

The analytical solutions for displacement w and moment M_r at the center including transversal shear effects are obtained for axisymmetric clamped plates [11,47] as follows:

$$w_{ref} = \frac{qR^4}{64D}(1 + \phi), \quad M_{ref} = \frac{qR^2}{16}(v + 3),$$

where

$$\phi = \frac{8}{3\kappa(1 - \nu)} \left(\frac{t}{R} \right)^2, \quad D = \frac{Et^3}{12(1 - \nu^2)}, \quad \kappa = \frac{5}{6}.$$

The results are reported in Table 8. We can see that the new method gives convergent results for a given plate thickness t , and yields uniform results with the a posteriori ratio r being close to 1 as t becomes small.

Acknowledgements

The work of the first author was partly supported by DFG Research Center MATHEON and the WCU program through KOSEF (R31-2008-000-10049-0). The second author would like to thank the Alexander von Humboldt Foundation for the support through the Alexander von Humboldt Fellowship during his stay at Department of Mathematics of Humboldt-Universität zu Berlin, Germany. Part of his work was also supported by the National Natural Science Foundation of China (10771150), the National Basic Research Program of China (2005CB321701), and the Program for New Century Excellent Talents in University (NCET-07-0584).

References

- [1] M. Amara, D. Capatina-papaghiuc, A. Chatti, New locking-free mixed method for the Reissner-Mindlin thin plate model, *SIAM J. Numer. Anal.* 40 (2002) 1561–1582.
- [2] D.N. Arnold, Discretization by finite elements of a model parameter dependent problem, *Numer. Math.* 37 (1981) 405–421.
- [3] D.N. Arnold, F. Brezzi, L.D. Marini, Locking-free Reissner-Mindlin elements without reduced integration, *Comput. Methods Appl. Mech. Engrg.* 196 (2007) 3660–3671.

- [4] D.N. Arnold, F. Brezzi, L.D. Marini, A family of discontinuous Galerkin finite elements for the Reissner–Mindlin plate, *J. Sci. Comput.* 22 (2005) 25–45.
- [5] D.N. Arnold, R.S. Falk, A uniformly accurate finite element method for the Reissner–Mindlin plate, *SIAM J. Numer. Anal.* 26 (1989) 1276–1290.
- [6] D.N. Arnold, D. Boffi, R.S. Falk, Approximation by quadrilateral finite elements, *Math. Comput.* 71 (2002) 909–922.
- [7] R. Ayad, G. Dhatt, J.L. Batoz, A new hybrid-mixed variational approach for Reissner–Mindlin plates: the MiSP model, *Int. J. Numer. Methods Engrg.* 42 (1998) 1149–1179.
- [8] I. Babuska, T. Scapolla, Benchmark computation and performance evaluation for a rhombic plate bending problem, *Int. J. Numer. Methods Engrg.* 28 (1989) 155–179.
- [9] K.J. Bathe, E.H. Dvorkin, A four-node plate bending element based on Mindlin–Reissner plate theory and mixed interpolation, *Int. J. Numer. Methods Engrg.* 21 (1985) 367–383.
- [10] J.L. Batoz, M. Benthahar, Evaluation of a new quadrilateral thin plate bending element, *Int. J. Numer. Methods Engrg.* 18 (1982) 1655–1677.
- [11] J.L. Batoz, G. Dhatt, *Modélisation des Structures par Éléments Finis, Poutres et Plaques*, vol. 2, Editions Hermès, Paris, 1990.
- [12] D. Braess, *Finite Elements: Theory, Fast Solvers, and Applications in Solid Mechanics*, Cambridge University Press, 2001.
- [13] J. Bramble, T. Sun, A negative-norm least squares method for Reissner–Mindlin plates, *Math. Comput.* 67 (1998) 901–916.
- [14] F. Brezzi, On the existence, uniqueness and approximation of saddle-point problems arising from Lagrange multipliers, *R.A.I.R.O Anal. Numer.* R2 (1974) 129–151.
- [15] K.J. Bathe, F. Brezzi, M. Fortin, Mixed-interpolated elements for Reissner–Mindlin plates, *Int. J. Numer. Methods Engrg.* 28 (1989) 1787–1801.
- [16] F. Brezzi, L. Marini, A nonconforming element for the Reissner–Mindlin plate, *Comput. Struct.* 81 (2003) 515–522.
- [17] F. Brezzi, M. Fortin, Numerical approximation of Mindlin–Reissner plates, *Math. Comput.* 47 (1986) 151–158.
- [18] F. Brezzi, M. Fortin, *Mixed and Hybrid Methods*, Springer-Verlag, 1991.
- [19] F. Brezzi, M. Fortin, R. Stenberg, Error analysis of mixed-interpolated elements for Reissner–Mindlin plates, *M²AS 1* (1991) 125–151.
- [20] Z. Cai, X. Ye, H. Zhang, Least-squares finite element approximations for the Reissner–Mindlin plate, *Numer. Linear Algebra Appl.* 6 (1999) 479–496.
- [21] C. Carstensen, J. Schöberl, Residual-based a posteriori error estimate for a mixed Reissner–Mindlin plate finite element method, *Numer. Math.* 103 (2006) 225–250.
- [22] S.-H. Chou, S. He, On the regularity and uniformness conditions on quadrilateral grids, *Comput. Methods Appl. Mech. Engrg.* 191 (2002) 5149–5158.
- [23] P.G. Ciarlet, *The Finite Element Method for Elliptic Problems*, North-Holland, 1978.
- [24] R. Duran, A. Ghioldi, N. Wolanski, A finite element method for the Mindlin–Reissner plate model, *SIAM J. Numer. Anal.* 28 (1991) 1004–1014.
- [25] R. Duran, E. Liberman, On mixed finite element methods for the Reissner–Mindlin plate model, *Math. Comput.* 58 (1992) 561–573.
- [26] R.S. Falk, T. Tu, Locking-free finite elements for the Reissner–Mindlin plate, *Math. Comput.* 69 (2000) 911–928.
- [27] L.P. Franca, R. Stenberg, A modification of a low-order Reissner–Mindlin plate bending element, in: J.R. Whiteman (Ed.), *The Mathematics of Finite Elements and Applications*, vol. VII, Academic Press, 1991, pp. 425–436.
- [28] J. Hu, Z.C. Shi, Two lower order nonconforming rectangular elements for the Reissner–Mindlin plate, *Math. Comput.* 76 (2007) 1771–1786.
- [29] T.J.R. Hughes, *The Finite Element Method: Linear Static and Dynamic Finite Element Analysis*, Prentice-Hall, 1987.
- [30] T.J.R. Hughes, L. Franca, A mixed finite element formulation for Reissner–Mindlin plate theory: uniform convergence of all higher order spaces, *Comput. Methods Appl. Mech. Engrg.* 67 (1988) 223–240.
- [31] C. Lovadina, A low-order nonconforming finite element for Reissner–Mindlin plates, *SIAM J. Numer. Anal.* 42 (2005) 2688–2705.
- [32] P.-B. Ming, Z.-C. Shi, Nonconforming rotated Q1 element for Reissner–Mindlin plate, *Math. Mod. Methods Appl. Sci.* 11 (2001) 1311–1342.
- [33] P.-B. Ming, Z.-C. Shi, Quadrilateral mesh revisited, *Comput. Methods Appl. Mech. Engrg.* 191 (2002) 5671–5682.
- [34] L.S.D. Morley, *Skew Plates and Structures*, Pergamon Press, Oxford, 1963.
- [35] J. Pitkäranta, Analysis of some low-order finite element schemes for Mindlin–Reissner and Kirchhoff plates, *Numer. Math.* 53 (1988) 237–254.
- [36] J. Pitkäranta, M. Suri, Design principles and error analysis for reduced-shear plate bending elements, *Numer. Math.* 75 (1996) 223–266.
- [37] R. Rannacher, S. Turek, Simple nonconforming quadrilateral Stokes element, *Numer. Methods Partial Diff. Eqn.* 8 (1992) 97–111.
- [38] A. Razaque, Program for triangular bending elements with derivative smoothing, *Int. J. Numer. Methods Engrg.* 6 (1973) 333–345.
- [39] T. Scapolla, Avoiding locking in Reissner–Mindlin plates with high-order hierarchic bubble plus finite elements, *J. Comput. Appl. Math.* 63 (1995) 291–299.
- [40] Z.-C. Shi, A convergence condition for the quadrilateral Wilson element, *Numer. Math.* 44 (1984) 349–361.
- [41] M. Suri, I. Babuska, C. Schwab, Locking effects in the finite element approximation of plate models, *Math. Comput.* 64 (1995) 461–482.
- [42] X.-P. Xie, T.-X. Zhou, Optimization of stress modes by energy compatibility for 4-node hybrid quadrilaterals, *Int. J. Numer. Methods Engrg.* 59 (2004) 293–313.
- [43] X.-P. Xie, T.-X. Zhou, Accurate 4-node quadrilateral elements with a new version of energy-compatible stress mode, *Commun. Numer. Methods Engrg.* 24 (2008) 125–139.
- [44] X. Ye, C. Xu, A discontinuous Galerkin method for the Reissner–Mindlin plate in the primitive variables, *Appl. Math. Comput.* 149 (2004) 65–82.
- [45] Z. Zhang, Analysis of some quadrilateral nonconforming elements for incompressible elasticity, *SIAM J. Numer. Anal.* 34 (1997) 640–663.
- [46] Z. Zhang, S. Zhang, Wilson element for the Reissner–Mindlin plate, *Comput. Methods Appl. Mech. Engrg.* 113 (1994) 55–65.
- [47] O.C. Zienkiewicz, R.L. Taylor, *The Finite Element Method*, Butterworth-Heinemann, Oxford, 2000.
- [48] G.-Z. Yu, X.-P. Xie, C. Carstensen, Uniform convergence and a posteriori error estimation for assumed stress hybrid finite element methods, submitted for publication.